FDG PET/CT for Rheumatic Diseases (Collagen Diseases)

6

Hiroyuki Yamashita, Chao Cheng, Xuena Li, Azusa Tokue, Kimiteru Ito, Kazuhiro Oguchi, Masatoyo Nakajo, and Noriko Oyama-Manabe

6.1 Role of FDG PET/CT in the Diagnosis of Rheumatic Diseases

Hiroyuki Yamashita

Abstract Advanced imaging techniques may enable early diagnosis and monitoring of therapy in various rheumatic diseases. To prevent irreversible tissue damage, inflammatory rheumatic disease must be diagnosed and treated in preclinical stages, requiring highly sensitive detection techniques. PET provides highly sensitive, quantitative imaging at a molecular level, revealing the important pathophysiological processes underlying inflammation. This section provides an overview of the current utility of FDG-PET/CT in patients with active rheumatic diseases such as rheumatoid arthritis (RA), polymyalgia rheumatica (PMR), spondyloarthritis (SpA), relapsing polychondritis (RPC), adult-onset Still's disease (AOSD), large vessel vasculitis (LVV), immunoglobulin G4-related disease (IgG4-RD), polymyositis/dermatomyositis (PM/DM), and Granulomatosis with polyangitis (GPA). We also discuss the role of FDG-PET/CT in the diagnosis and monitoring of these diseases.

Keywords: Rheumatoid arthritis (RA), Polymyalgia rheumatica (PMR), Spondyloarthritis (SpA), Relapsing polychondritis (RPC), Adult-onset Still's disease (AOSD), Large vessel vasculitis (LVV), Immunoglobulin G4-related disease (IgG4-RD), Polymyositis/dermatomyositis (PM/DM), Granulomatosis with polyangitis (GPA), FDG-PET/CT

6.1.1 Introduction

Timely diagnosis and early effective treatment can improve the outcome of various inflammatory rheumatic diseases [1]. To enable early diagnosis and individualized therapeutic protocols, sensitive monitoring tools such as advanced imaging techniques are needed. Promising results have already been obtained using anatomical imaging modalities, such as MRI and ultrasound (US), which allow highly sensitive detection of synovitis and bone marrow edema in inflammatory arthropathies and vascular thickening in systemic vasculitis [2–5]. Each technique, however, has drawbacks and limitations; MRI usually produces images within a limited field of view, and US is limited by variability and labor intensity. In addition, in the presence of inflammation, both techniques can visualize indirect inflammatory signs such as increased tissue water content and hyperperfusion. Because diagnosis and assessment of disease activity at subclinical stages is

H. Yamashita (✉)
Division of Rheumatic Diseases, National Center for Global Health and Medicine, Tokyo, Japan
e-mail: hiroyuki_yjp2005@yahoo.co.jp

C. Cheng
Shanghai Changhai Hospital, Shanghai, China
e-mail: chao_cheng_1999@163.com

X. Li
Department of Nuclear Medicine, The First Hospital of China Medical University, Shenyang, Liaoning Province, China
e-mail: lixuenacmunm@163.com

A. Tokue
Department of Diagnostic Radiology and Nuclear Medicine, Gunma University Hospital, Maebashi, Gunma, Japan
e-mail: azut@gunma-u.ac.jp

K. Ito
Department of Diagnostic Radiology, National Cancer Center Hospital, Tokyo, Japan
e-mail: kimito@ncc.go.jp

K. Oguchi
Positron Imaging Center, Aizawa Hospital, Matsumoto, Nagano, Japan
e-mail: pet-dr@ai-hosp.or.jp

M. Nakajo
Department of Radiology, Graduate School of Medical and Dental Sciences, Kagoshima University, Kagoshima, Japan
e-mail: toyo.nakajo@dolphin.ocn.ne.jp

N. Oyama-Manabe
Department of Diagnostic and Interventional Radiology, Hokkaido University Hospital, Sapporo, Hokkaido, Japan
e-mail: norikooyama@med.hokudai.ac.jp

H. Toyama et al. (eds.), *PET/CT for Inflammatory Diseases*, https://doi.org/10.1007/978-981-15-0810-3_6

increasingly important, nuclear imaging techniques are becoming more widely used.

FDG is used to trace glucose metabolism. Many cancer cells showed elevated expression of glucose transporters and hexokinase. Most cancer cells are FDG avid, and a fusion imaging technique combining PET/CT, which provides information on both anatomy and glucose metabolism, has improved the diagnostic accuracy and is now widely used in oncology. FDG uptake is not limited to cancer cells; uptake may also occur in various inflammatory cells. Elevated FDG uptake by activated macrophages and by newly formed granulation tissue was demonstrated by Kubota et al. in the early 1990s [6, 7]. The uptake of FDG by cancer cells is postulated to involve the same mechanism as in inflammatory cells. Cramer et al. reported that HIF1α activation is essential for myeloid cell (granulocytes and monocytes/macrophages) infiltration and activation an in vivo inflammation model [8]. More recently, Matsui et al. reported FDG uptake in the area in which inflammatory cell infiltration and synovial cell hyperplasia were visible in an arthritis model. Based on in vitro experiments, Matsui et al. suggested that the cell types responsible for FDG uptake are activated macrophages and proliferating fibroblasts in the presence of cytokine stimulation and under hypoxic circumstances within a joint [9]. The FDG uptake by inflammatory tissue, such as arthritis lesions, seems to reflect the inflammatory activity accurately.

Such studies have strongly encouraged the clinical application of FDGPET/CT for rheumatic diseases.

6.1.2 Rheumatoid Arthritis (RA)

RA is a symmetric, inflammatory, peripheral polyarthritis of unknown etiology. It typically leads to deformity through the stretching of tendons and ligaments and destruction of joints through the erosion of cartilage and bone. If it is untreated or unresponsive to therapy, inflammation and joint destruction lead to loss of physical function, inability to carry out daily tasks of living, and difficulties in maintaining employment. Therefore, early diagnosis of RA and evaluation of latent activity are important, and FDG-PET/CT may be useful for this purpose.

In 1995, the first FDG-PET studies in active RA patients revealed increased ^{18}F-FDG uptake in clinically inflamed wrist joints. Further, standardized uptake values (SUVs) for ^{18}F-FDG were correlated with clinical indicators such as tenderness and swelling [10]; these findings were confirmed in other studies [11, 12]. ^{18}F-FDG SUV data in arthritis is also correlated with disease activity score 28 (DAS28) and simple disease activity index (SDAI) values. The number of FDG-positive joints is also strongly correlated with their cumulative SUV and disease duration [11]. However, Kubota et al. [12] and Goerres et al. [13] found that simple visual semiquantitative scoring from 0 to 4 based on ^{18}F-FDG joint uptake [12] also reflected clinical evidence of inflammation in joints. This approach eliminates the need to quantify tracer uptake and makes the technique more accessible to routine clinical practice.

Beckers et al. [11] reported sensitivities of up to 90% in a study evaluating 356 joints of 21 established RA patients using ^{18}F-FDG PET. In this study, visually identified FDG positivity was clearly associated, according to odds ratios, with both joint swelling and tenderness. Regarding specificity, ^{18}F-FDG PET allows excellent differentiation between inflamed and healthy joints, both among RA patients and between patients and healthy controls; healthy joints do not take up the tracer at all [11, 14]. However, despite a greater number of FDG-positive joints in RA than in osteoarthritis patients, absolute values for tracer uptake do not differ between these two conditions [15]. Nonetheless, whole-body PET may aid in differentiation between RA and other inflammatory joint diseases, as differences in bio-distribution patterns have allowed distinction between some forms of arthritis associated with connective tissue disease [16].

Although clinical treatment response is not correlated with semiquantitative PET measures, ^{18}F-FDG PET images do detect reductions in metabolism and treatment-related changes in the volume of pannus that are not detectable with conventional imaging [10]. In 2006, Beckers et al. [17] used ^{18}F-FDG PET to image joints before and after anti-TNF therapy and found that that PET-positivity was correlated with higher SUVs. In contrast, ^{18}F-FDG PET revealed no significant metabolic changes following acupuncture treatment of affected knees in six chronic RA patients [18].

Several studies have indicated that subclinical disease is present during clinical remission and may be related to progression of joint damage [19]. Due to its high sensitivity and ability to scan multiple joints in one session, PET may allow detection of such subclinical disease activity. Whole-body PET scanning in 18 RA patients, four of whom were in remission [10], showed significant differences between those with active arthritis and those in clinical remission [12]. ^{18}F-FDG uptake by large joints, total visual PET scores for involved joints, SUV_{max}, and the mean number of joints per patient with high FDG uptake were all significantly lower for patients in clinical remission. In all patients in remission, however, increased ^{18}F-FDG uptake was still observed in one or more joints, suggesting subclinical disease activity.

Besides its ability to detect and monitor subclinical disease, PET may also have prognostic power. Recently, ^{18}F-FDG changes in inflamed hand joints after 2 weeks of infliximab treatment were correlated with DAS28 joint scores at 14–22 weeks of treatment [20]. In contrast, erythrocyte sedimentation rate (ESR), C-reactive protein (CRP),

and DAS28 scores had no such predictive value after 2 weeks of therapy.

A number of studies have examined the ability of PET to accurately indicate treatment outcomes compared to MRI. Before and during treatment with nonsteroidal anti-inflammatory drugs (NSAIDs), prednisone, or methotrexate, changes in joint uptake of ^{18}F-FDG, as revealed by PET, were strongly correlated with synovial volume upon MRI in RA patients [10, 21]. Comparison of semiquantitative PET data with US data and clinical findings [11] revealed a significant linear correlation between SUVs and synovial thickness, as measured by US, for nearly all joints. This relationship was stronger for larger joints, as these are more accurately evaluated by semiquantitative scoring [22]. Moreover, some small joints in the hand cannot easily be evaluated in three dimensions by US for anatomical reasons [23]. The first study simultaneously investigating PET, MRI, and US in RA patients showed that enhanced FDG uptake was associated with positive findings obtained by the other two imaging techniques. In addition, the study also revealed correlations among SUVs from PET, relative contrast enhancement from MRI, and synovial thickness from US. Changes in SUVs in RA-affected knees after initiation of anti-TNF therapy were also correlated with changes in MRI parameters and serum CRP and metalloproteinase-3 (MMP-3) levels, but not with changes in synovial thickness as measured via US [17].

Hybrid PET-CT and PET-MRI have become available. Combining PET with CT has helped place pathophysiologic PET information in its anatomic context [24]. Thus, hybrid imaging should allow more precise localization of PET signals and PET-MRI should limit radiation exposure [25].

Recent reports have demonstrated that a higher baseline SUV for joints correlate with a higher risk for subsequent joint damage [26, 27].

6.1.3 Polymyalgia Rheumatica

PMR is an inflammatory rheumatic disease characterized by aches and morning stiffness in the shoulders, hip girdle, and neck in patients over 50 years of age. PMR is diagnosed by the exclusion of other disorders causing similar complaints and by its rapid response to low-dose corticosteroid therapy [28, 29]. Although its pathology is unknown, synovitis and bursitis are common features of this disease. MRI and US frequently reveal inflammation of the tenosynovial sheaths of patients' hands or feet [30–32].

Moosig et al. [33] quantified FDG accumulation in large vessels in 13 untreated patients with PMR by PET, and compared these data with serological markers of inflammation. By visual evaluation, FDG uptake by the aorta or its major branches increased in 12 of 13 patients. In active PMR, the mean region of interest (ROI) index for all vascular regions exceeded that of controls by 70%. Among the eight patients who underwent follow-up PET, this index declined substantially. In active PMR, FDG uptake was significantly correlated with CRP, ESR, and platelet counts. The observed FDG accumulation in the aorta and its branches and the strong correlation between tracer uptake and markers of inflammation suggests that large vessel arteritis is characteristic of active PMR.

Brockmans et al. [34] investigated whether FDG deposition in various vascular lesions and large joints of patients with isolated PMR predicts relapse. All patients underwent an FDG-PET scan before steroid treatment and at 3 and 6 months; seven vascular areas were scored and a total vascular score (TVS) was calculated, ranging from 0 to 21. At diagnosis, vascular FDG uptake was noted in 31% of patients, predominantly at the subclavian arteries. FDG uptake in the shoulders was noted in 94% of patients, in the hips in 89%, and in the spinous processes of the vertebrae in 51%. FDG uptake intensity was not correlated with the risk of relapse in either the large vessels or large joints.

While Brockmans et al. [34] analyzed FDG-PET changes in patients with PMR, we analyzed the precise distribution of lesions via PET/CT and evaluated differences in FDG accumulation between PMR and similar diseases. In PMR patients, FDG uptake was increased in ischial tuberosities, greater trochanters, and lumbar spinous processes [35]. Positive results at two or more of these sites were highly sensitive (85.7%) and specific (88.2%) for the diagnosis of PMR, and shoulder or hip joint involvement were not disease-specific. High FDG accumulation was found in the aortas and subclavian arteries of two PMR patients in whom FDG uptake did not identify temporal arteritis or scanty synovium and perisynovium. PET/CT images of the 12 PMR patients without apparent vascular involvement revealed synovitis and/or perisynovitis.

Furthermore, we compared PET/CT findings in a large number of PMR cases with those in patients with elderly-onset RA (EORA), which is extremely difficult to distinguish from PMR. We observed no significant difference in FDG uptake in the shoulders or hips. However, specific uptake patterns were observed in each group: circular and linear uptake patterns around the humeral head in EORA, and focal and nonlinear uptake patterns in PMR. Moreover, focal uptake at the front of the hip joint, indicating iliopectineal bursitis, tended to be limited to the PMR group. The sensitivity and specificity for PMR diagnosis were very high at 92.6% and 90.0%, respectively, when at least three of the five items, including findings characteristic of shoulder and iliopectineal bursitis, FDG uptake in ischial tuberosities and spinal spinous processes, and lack of FDG uptake in the wrists, were satisfied. FDG-PET/CT may be useful for the detection of PMR lesions, which are difficult to identify using other methods [36].

Subsequently, several papers on PET findings in PMR were published. Based on a detailed analysis of PET findings in knee joints with PMR, Cimmino et al. hypothesized that capsulitis is the source of inflammation [37]. Wakura et al. hypothesized that not only bursitis but also enthesitis may be the main cause of lesions and that these conditions may have developed from synovitis and inflammation of the surrounding area [38]. Owen et al. demonstrated that hamstring peritendonitis is a typical manifestation of PMR on PET/CT [39]. Rehak et al. comprehensively examined PET results from the affected site of PMR and roughly divided the sites into large arteries (V), proximal joints (A), and extraarticular synovial structures (E). The authors also demonstrated that PMR can be classified into six types: A (alone), E (alone), A + E, A + V, E + V, and A + E + V [40]. Furthermore, an increase in praepubic FDG uptake was also shown to be typical in PMR [41]. Praepubic inflammation is probably related to enthesitis and tenosynovitis at the origin of pectineus and adductor longus muscles ventrally from the pubis. Camellino et al. compared the PET findings and clinical symptoms of PMR and demonstrated that the clinical symptoms do not always correlate with the findings of cervical and lumbar interspinous bursitis [42]. Palard–Novello et al. compared the PET findings in PMR before and after treatment with Tocilizumab and demonstrated its usefulness in evaluating disease activity [43].。 .

6.1.4 Spondyloarthritis (SpA)

SpA includes ankylosing spondylitis (AS), psoriatic arthritis (PsA), reactive arthritis (ReA), enteropathic arthritis, and undifferentiated spondyloarthritis (uSpA) [44]. SpA often involves enthesitis, sacroiliitis, and inflammatory spondylitis [45].

Taniguchi et al. [46] evaluated the accuracy of FDG-PET/CT in detecting enthesitis in patients with SpA. PET/CT scans of the shoulder, hip, and knee joints revealed that FDG accumulates at the entheses in SpA and in the synovium in RA patients. SUV_{max} was significantly higher at the entheses of the lumbar spinous process, pubic symphysis, and ischial tuberosity in SpA patients than in RA patients. Lumbar spinous processes and ischial tuberosities appeared more frequently via PET/CT than MRI in SpA patients. They concluded that PET/CT represents an alternative modality to identifying enthesitis, and will likely contribute to the early diagnosis of SpA.

Strobel et al. [47] evaluated the performance of FDG-PET/CT for the diagnosis of sacroiliac joint (SIJ) arthritis in patients with active AS using patients with mechanical low back pain (MLBP) as a control. The mean ratio of FDG uptake in the SIJ to that in the sacrum in AS patients was 1.66, while that in MLBP patients was 1.12. With plain radiography as the gold standard and using an SIJ/S ratio of 1.3 as the threshold, the sensitivity and specificity of FDG-PET/CT for arthritis were 80% and 77%, respectively. On a per-SIJ basis, the greatest sensitivity (94%) was found in grade 3 sacroiliitis. These results suggest that quantitative FDG-PET/CT may be useful to diagnose sacroiliitis in active AS, providing an alternative to conventional bone scintigraphy in times of molybdenum shortage.

We used FDG-PET/CT to compare SUVs in various joints in 53 patients with SpA, PMR, and RA [48]. In PMR patients, the SUV_{max} for ischial tuberosities was significantly higher than in SpA or RA patients, and those in the greater trochanter and spinous processes were also significantly higher than in RA patients. In SpA patients, SUV_{max} in the SIJ was greater than in PMR or RA patients. No significant difference in vertebral scores was observed among groups. PET/CT findings can thus distinguish SpA from RA and PMR and are useful for the early diagnosis of sacroiliitis.

Vijayant et al. [49] evaluated the potential of FDG-PET in the early assessment of treatment response in various rheumatic diseases, including 11 newly diagnosed SpA patients and one patient with PsA. In the SpA group, FDG uptake in the affected joint was heterogeneous, low grade, and non-symmetrical, with intense tendon and muscular uptake in symptomatic joints. In contrast, FDG uptake in the PsA patient was intense in the joints and soft tissue. If larger studies corroborate these findings, FDG-PET could be useful to distinguish RA from SpA. FDG-PET also appears to be a sensitive tool in the early assessment of treatment response, especially when using quantitative information.

Subsequently, several papers on SpA and PET were published. Bruijnen et al. argued that unlike for RA, PET/CT is not as useful for AS from the perspective of evaluating activity. The authors argued that the activity of AS is reflected by ossification rather than inflammation in PET/CT [50]. Meanwhile, Lee et al. argued that not only syndesmophyte in the spine of patients with AS but also inflammatory lesions are associated with active bone synthesis, as evaluated by FDG uptake [51]. Based on a study concerning active AS using hybrid PET/MRI, Buchbender et al. hypothesized that bone marrow edema rather than chronic changes is more closely associated with osteoblastic activity. The authors reported that the accumulation of FDG was due to bone marrow edema and fat deposition [52]. Takata et al. discovered that asymptomatic enthesitis can be identified in PsA patients based on PET/CT images; further, they indicated that there are more cases of asymptomatic PsA than previously expected [53]. Chaudhari et al. evaluated PsA-affected hands and wrist joints using high-resolution FDG–PET/CT and reported that the technique is useful in the quantitative evaluation of disease activity (synovitis, enthesitis, edema, and bone fracture) [54]. Idolazzi et al. performed PET/CT in patients with AS and confirmed a correlation between the

number of FDG-positive sites and disease activity. They also argued that PET/CT may be a useful tool for follow-up evaluations of AS [55]. Based on their results, Park et al. stated that FDG-PET may be useful in identifying patients with AS at a higher risk for future syndesmophyte formation [56]. Based on dual-phase PET/MRI findings of sacroiliac joints in patients with AS, Sawicki et al. reported a possibility that regional hyperemia and osteoblast activity, and not chronic AS lesions, are associated with inflammation [57].

6.1.5 Relapsing Polycondritis (RPC)

Relapsing polychondritis (RPC) is an immune-mediated condition associated with inflammation in cartilaginous structures and other tissues throughout the body, particularly the ears, nose, eyes, joints, and respiratory tract. The clinical features and course of RPC vary considerably from patient to patient. Subtle, early manifestations often remain unrecognized for prolonged periods. As a result, the diagnosis is frequently obtained only after the emergence of classic features such as auricular inflammation, saddle-nose deformity, or other features of cartilage destruction.

We first investigated the utility of FDG-PET/CT for the diagnosis and evaluation of disease activity in five RPC patients undergoing FDG-PET/CT in our hospital and eight cases in the literature [58]. Typical FDG accumulation was noted in tracheobronchial trees, costal cartilage, joints, larynx, nasal cavity/paranasal sinuses, auricles, lymph nodes, and the aorta. In one patient, PET revealed nasal chondritis despite an absence of nasal changes upon physical examination. Of five patients with costochondritis, four remained asymptomatic. Of the nine patients with airway FDG accumulation, eight developed respiratory symptoms and all had CT abnormalities. In the remaining patient, airway FDG accumulation was evident despite the absence of airway symptoms and a lack of abnormalities in the respiratory function test or CT. PET also revealed bronchial chondritis in asymptomatic patients. In the five patients examined by PET posttreatment, FDG accumulation diminished as symptoms improved and inflammation decreased. We conclude that FDG-PET/CT is a potentially powerful tool for the early diagnosis of RPC, especially in patients with affected organs that are difficult to biopsy. This modality also facilitates the evaluation of the extent of disease and disease activity during treatment.

Subsequently, Lei et al. conducted a similar study and reported similar findings [59].

6.1.6 Adult Onset of Still Disease (AOSD)

Adult-onset Still's disease (AOSD) is a systemic inflammatory disease of unknown etiology and pathogenesis. It is characterized by fever, skin eruptions, systemic organ involvement, and arthralgias. Arthralgias and arthritis occur in the majority of patients with AOSD, with incidences ranging from 69 to 96%. Hepatosplenomegaly is also often seen in this disease. Frequency of hepatomegaly and splenomegaly has been reported to be 18.2–50.0% and 18.2–57.0%, respectively, and the frequency of increased liver enzyme was 63.6–84.0%. The diagnosis of AOSD remains a clinical diagnosis. It is difficult to diagnose because of its low prevalence, heterogeneous clinical manifestations, and absence of pathognomic clinical features. The disease also lacks a specific diagnostic test. Before the final diagnosis of AOSD is made in suspected subjects, it is important to rule out a wide range of other diseases including infectious diseases, malignancies, and rheumatic diseases.

We first evaluated FDG-PET/CT for diagnosis and disease evaluation of AOSD by investigating FDG uptake for characteristic findings in seven patients with AOSD and reviewing the literature on seven previous reports of PET/CT in AOSD patients [60]. FDG accumulation was positive mainly in the bone marrow (100%), spleen (90.9%), lymph nodes (80.0%), and joints (75.0%). In addition, FDG uptake was positive in the pericardium, pleura, salivary glands, eyelids, muscle, and major blood vessels. Follow-up PET/CT showed diminished FDG accumulation, as measured by SUV_{max}, in the bone marrow, spleen, and lymph nodes. The only correlation with laboratory data was between lactate dehydrogenase (LDH) and spleen SUV. In conclusion, FDG-PET/CT is useful for long-term assessment of AOSD activity in individual patients. However, PET/CT findings alone are not sufficient to make a differential diagnosis of AOSD versus malignant lymphoma.

Subsequently, Dong et al. conducted a similar study and reported somewhat similar findings [61].

6.1.7 Large-Vessel Vasculitis (LVV)

Large-vessel vasculitis (LVV) can be clinically diagnosed and classified according to specific criteria. During the Chapel Hill Conference in 2012, two forms of primary LVV were distinguished: giant cell arteritis (GCA) and Takayasu arteritis (TAK). Early diagnosis and assessment of the extent of LVV are crucial factors for adequate therapeutic management. LVV diagnosis is often difficult because of the absence of specific symptoms and signs and the limited specificity of the available biochemical tests. Morphological imaging techniques such as angiography, CT, MRI, and US cannot detect the early phase of inflammation of the vessel wall because of slight anatomical changes at this time. It is also difficult to distinguish active inflammatory lesions from the residual anatomical changes of scarring.

From a systematic review on FDG-PET/CT in patients with LVV, Treglia et al. [62] drew several conclusions. First, FDG-PET/CT appears to be useful in early diagnosis and in the assessment of disease activity and extent. Second, the correlation between FDG-PET findings and serological inflammatory markers, as well as the usefulness of FDG-PET/CT in evaluating treatment response, require further investigation. Additionally, FDG-PET/CT appears to be superior to conventional imaging methods, such as US or MRI, in the diagnosis of LVV, but not in assessing response to immunosuppressive treatment, predicting relapse, or evaluating vascular complications. Lastly, PET analysis and diagnostic criteria should be standardized to allow reproducible, directly comparable results.

We also studied the usefulness of FDG-PET/CT and contrast-enhanced CT in early diagnosis and treatment follow-up of patients with LVV presenting as elderly-onset inflammation of unknown origin (IUO) [63]. For quantitative comparison, we evaluated SUV_{max} and PET scores of the aortic wall, as well as aortic wall thickness (W) and its ratio with respect to aortic radius (W/R) by contrast-enhanced CT, and compared pretreatment and posttreatment values. Of 124 patients who were hospitalized due to advanced age and IUO, 10.5% had LVV, and more than half had nonspecific symptoms. Compared to control subjects, patients with LVV showed significantly higher aortic wall SUV_{max}, higher PET scores as revealed by FDG-PET/CT, and increased aortic wall thicknesses as revealed by contrast-enhanced CT. PET scores and contrast-enhanced CT revealed significant reductions in aortic wall thickness following treatment. In conclusion, LVV is an important cause of IUO with nonspecific symptoms in elderly patients. Combined contrast-enhanced CT and FDG-PET/CT is useful for early diagnosis and early treatment evaluation of LVV, as it detects amelioration of aortic wall thickening.

Notably, FDG-PET/CT may be negative for old lesions even if the arterial stricture is severe. Lesions in which the inflammatory activity has already subsided may not be appropriate for evaluation by FDG-PET; in such cases, morphological imaging such as MRI or contrast-enhanced CT may be used. Again, LVV should be diagnosed in the early phase with FDG-PET/CT to prevent stricture formation.

6.1.8 Immunoglobulin G4-Related Disease (IgG4-RD)

IgG4-RD is a systemic disorder associated with lesions characterized by mass formation in multiple specific organs. This disorder comprises Mikulicz's disease (MD), autoimmune pancreatitis (AIP), hypophysitis, Riedel thyroiditis, interstitial pneumonitis, interstitial nephritis, lymphadenopathy, retroperitoneal fibrosis, and inflammatory pseudotumor [64]. The combination of such lesions on FDG-PET/CT may strongly suggest or support the diagnosis of IgG-4RD.

Shigekawa et al. noted that the FDG-PET pattern at baseline, including extra-abdominal lymph nodes and/or salivary glands and the involvement of the eyes and biliary ducts, can be useful for discriminating between AIP and pancreatic cancer [65]. Ozaki et al. also found that FDG uptake by hilar lymph nodes was significantly more frequent in AIP than in pancreatic cancer and reported that uptake by the lacrimal gland, salivary gland, biliary duct, retroperitoneal space, and prostate were seen only in AIP [3]. They reported that a longitudinal pattern, heterogeneous accumulation, and multiple localizations in the pancreas indicated AIP rather than pancreatic cancer [66].

Ebbo et al. [67] evaluated FDG-PET/CT for disease staging and treatment evaluation in 46 FDG-PET/CT images from 21 IgG4-RD patients. At diagnosis or relapse, all patients presented abnormal FDG uptake at sites typically affected by IgG4-RD. In most cases, FDG-PET/CT was more sensitive than conventional imaging to detect organ involvement, especially in the arteries, salivary glands, and lymph nodes. In a few cases, FDG-PET/CT failed to identify small or contiguous lesions in the brain or kidneys. Evaluation before and after treatment showed that FDG-PET/CT results were generally correlated with treatment response and disease activity. This retrospective study shows that FDG-PET/CT imaging is useful for staging IgG4-RD and assessing treatment response.

In addition, we evaluated the utility of FDG-PET/CT in eight IgG4-RD patients [68]. Although nearly all patients were negative for CRP, various organs took up significant amounts of FDG. In conclusion, FDG accumulation in organs characteristically affected by IgG4-RD allows diagnosis without evidence of an associated inflammatory reaction.

Subsequently, several similar reports showed the utility of FDG–PET/CT in IgG4-RD [69–73]. Berti et al. examined the relationship between IgG4-RD disease activity and FDG uptake and reported that FDG accumulation in IgG4-RD reflects perturbations in the B-cell compartment. The authors concluded that PET is a reliable method for evaluating IgG4-RD disease activity [74]. Takano et al. compared the PET findings of patients with and those suspected of having IgG4-related sclerosing sialadenitis (IgG4-SS) and argued that IgG4-SS may be noninvasively diagnosed by reviewing the PET findings in addition to serum IgG4 level and clinical findings [75].

6.1.9 Polymyositis/Dermatomyositis (PM/DM)

Polymyositis (PM) and dermatomyositis (DM) are idiopathic inflammatory myopathies, characterized by the shared features of proximal skeletal muscle weakness and evidence of muscle inflammation. DM, unlike PM, is associated with a variety of characteristic skin manifestations. The association between malignancy and inflammatory myopathy has been supported by numerous epidemiologic studies, with the strongest association occurring in those with DM.

Owada et al. [76] examined whether FDG-PET can detect myositis or extramuscular lesions in patients with PM and DM, and observed increased FDG uptake in muscle in 33% of patients. The sensitivity of FDG-PET to detect myositis was lower than that of electromyography (EMG), MRI, and muscle biopsy, and patients with and without increased FDG uptake in muscle did not differ clinically, although those with FDG muscle uptake had a tendency toward extended myositis with endomysial cell infiltration. In contrast, FDG-PET did detect neoplasms in patients with associated malignancy, which accounted for 38.9% of patients with interstitial lung disease. Thus, FDG-PET imaging appears to have limited usefulness for the evaluation of myositis in patients with PM and DM because of its low sensitivity.

On the other hand, Tanaka et al. [77] also conducted a retrospective study to determine whether FDG-PET/CT discriminates PM and DM from nonmuscular diseases and whether FDG uptake in proximal muscles reflects severity of muscular inflammation. Mean proximal muscle SUVs were significantly greater in PM and DM patients than in controls and were correlated with mean proximal manual muscle test scores and serum creatine kinase and aldolase levels. Furthermore, SUVs in proximal muscles from which biopsy specimens were obtained were significantly correlated with histological grade for inflammatory cell infiltration. These results suggest that FDG-PET/CT is useful in the diagnosis of PM and DM when inflammation in proximal muscles is also quantitatively assessed by other means. These results also indicate that local FDG uptake reflects inflammatory activity in proximal muscle and can help guide biopsy site selection.

Several studies concerning PET findings in inflammatory myositis have been reported, and all of their results suggest a correlation between myositis disease activity and the FDG accumulation degree [78–81]. In particular, Matuszak et al. reported that screening for malignant tumors was useful [78], whereas Motegi et al. noted that FDG-PET was useful in evaluating the activity of interstitial pneumonia with myositis [79].

6.1.10 Granulomatosis with Polyangitis (GPA)

Wegener's granulomatosis (WG), namely granulomatosis with polyangiitis (GPA), is a relatively rare disease characterized by granulomatous necrotising vasculitis. In the first evaluation of FDG-PET/CT imaging for the diagnosis and monitoring of WG [80], we retrospectively analyzed 13 FDG-PET/CT images obtained from eight patients. WG lesions of the upper respiratory tract and lung were more clearly detected by FDG-PET/CT fusion imaging than by nonenhanced CT alone, and all active lesions showed decreased FDG uptake after treatment. In addition, FDG-PET/CT can be combined with other imaging methods to inform selection of biopsy sites. In conclusion, FDG PET/CT is a feasible modality for evaluating lesion activity and therapeutic efficacy in WG.

Several research studies on PET findings in GPA have been published. Similar to the aforementioned reports, FDG–PET/CT was indicated as useful in identifying lesions and biopsy sites as well as evaluating disease activity [81–83]. Some reports also stated that the FDG-PET was useful in evaluating inflammation in aortitis as a complication of GPA [84].

6.1.11 Conclusion

FDG-PET/CT can provide information on active inflammatory lesions. It is a very sensitive but nonspecific imaging modality. The distribution patterns of inflammatory foci sometimes suggest specific disease. In general, if FDG-PET/CT imaging is used appropriately, it may provide very helpful information for accurate diagnosis, particularly for identification of biopsy sites. In addition, FDG-PET/CT is very sensitive for monitoring disease activity. It could be applied to the prediction of therapeutic response, but further studies are required. FDG-PET/CT is a promising imaging modality for rheumatic diseases.

6.2 Adult-Onset Still's Disease

Chao Cheng

Abstract The diagnosis of adult-onset Still's disease (AOSD) is nonspecific and requires the exclusion of other diseases including infectious, inflammatory and malignant diseases. AOSD has been referred to as the archetypal febrile autoinflammatory illness. It typically causes a diurnal fever, highest in the evening accompanied by a salmon-pink rash and arthralgia, with both the fever and rash subsiding completely within hours. Currently, the diagnosis is largely clinical due to low prevalence, vague symptoms and the absence of any diagnostic test. AOSD is the archetypal febrile autoimmune disease.

Keywords: Adult-onset Still's disease, FDG, PET/CT, Lymph nodes

6.2.1 Clinical Presentation

A 33-year-old female known with intermittent fever (T_{max} of 39 °C) for more than 10 days without obvious incentives. The rash was widely located in the skin of hip and arm, with obvious pharynx and body sore. The patient had no chills, no cough. Laboratory examination found: WBC, 10.6×10^9/L; NEUT, 10.08×10^9/L; ESR, 44 mm/H; CRP, 129 mg/L; PCT,0.228 ng/mL; ANA (negative); ALT, 1004 U/L; AST,893 U/L; IgE, 255.00 IU/mL.

6.2.2 Key Images

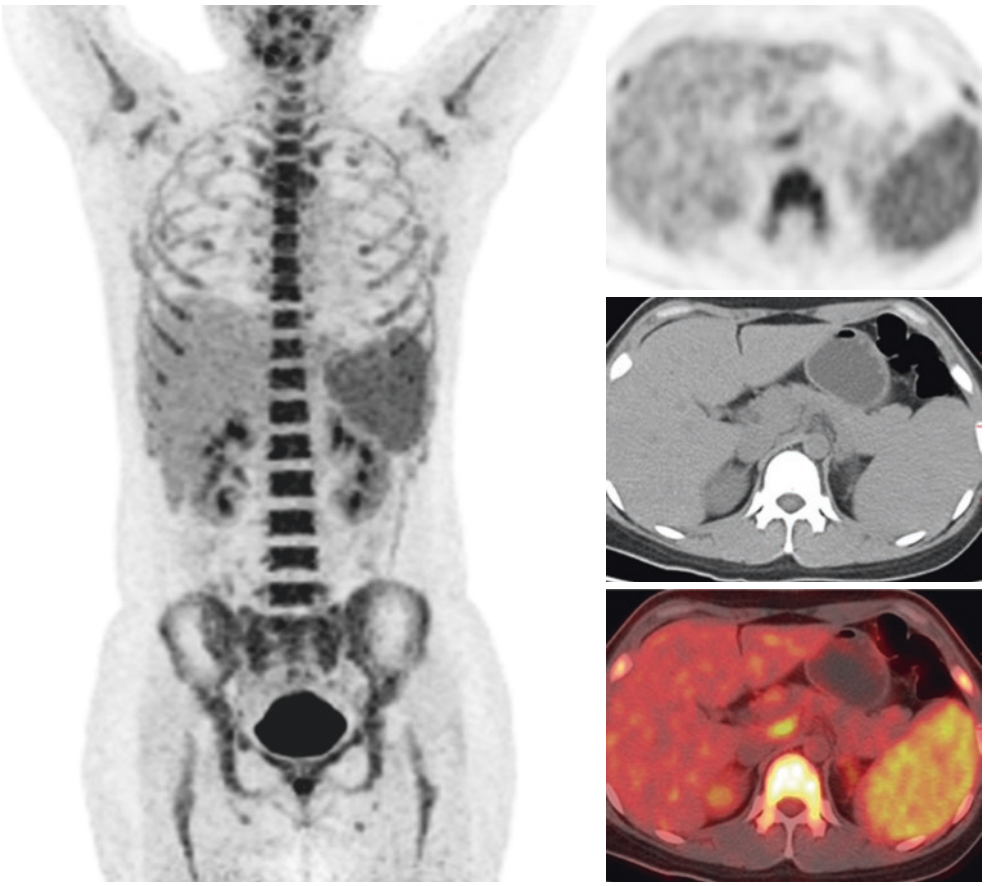

Fig. 6.1 Demonstrate increased FDG uptake for ^{18}F-FDG PET/CT images in the bone (SUV_{max} = 7.7), spleen (SUV_{max} = 4.0) and multiple lymph nodes (SUV_{max} = 4.5)

6.2.3 Technique

- Patient preparation: patient should not take anything by mouth for 6 h before administration of radiopharmaceutical.
- 344 MBq of F18-FDG administered intravenously (body weight = 65 Kg).
- Imaging device: whole body PET/CT camera (Siemens biograph 64) with resolution of 4.0 mm FWHM.

6.2.4 Differential Diagnosis

- Malignant lymphoma,
- Tuberculosis,
- Metastatic tumor.

6.2.5 Diagnosis and Clinical Follow-Ups

The patient received anti-inflammatory therapy (Methylprednisolone, Hydroxychloroquine, Human Immumoglobulin) and recovered promptly.

6.2.6 Discussion

AOSD is a chronic systemic inflammatory disease. Due to the nonspecific features in clinical performance, laboratory tests, and imaging modalities, AOSD remains difficult to diagnose. FDG-PET/CT has been suggested to be useful for AOSD diagnosis and evaluation of disease activity [60, 85]. Especially grossly 18F-FDG accumulation in the bone marrow and spleen is considered to be a characteristic of AOSD. Although the definitive diagnosis cannot be made based only on FDG-PET/CT findings in a case with suspected AOSD, these findings are extremely useful as support for the diagnosis [86].

6.3 Polymyositis/Dermatomyositis

Chao Cheng

Abstract Idiopathic inflammatory myopathies are a heterogeneous group of disorders clinically characterized by progressive proximal muscle weakness and pathologically by mononuclear cell infiltration and fiber necrosis in muscles. Polymyositis (PM), dermatomyositis (DM) and inclusion body myositis are representative phenotypes. PM/DM can present with prominent truncal muscle weakness or preferential involvement of respiratory muscles. We can visually evaluate the extent and pattern of muscle lesions systemically by F-18 FDG PET/CT.

Keywords: Polymyositis, Dermatomyositis, FDG, PET/CT

6.3.1 Clinical Presentation

A 41-year-old man known with Intermittent limb muscle soreness for more than 1 year, increased in the past week and accompanied by limb weakness. Electromyogram examination suggests myogenic damage. Laboratory examination found: CK, 5537 U/L; CKMB 61.0 U/L, LDH 226 U/L, K^+, 1.9 mmol/L. The levels of tumor markers were normal.

6.3.2 Key Images

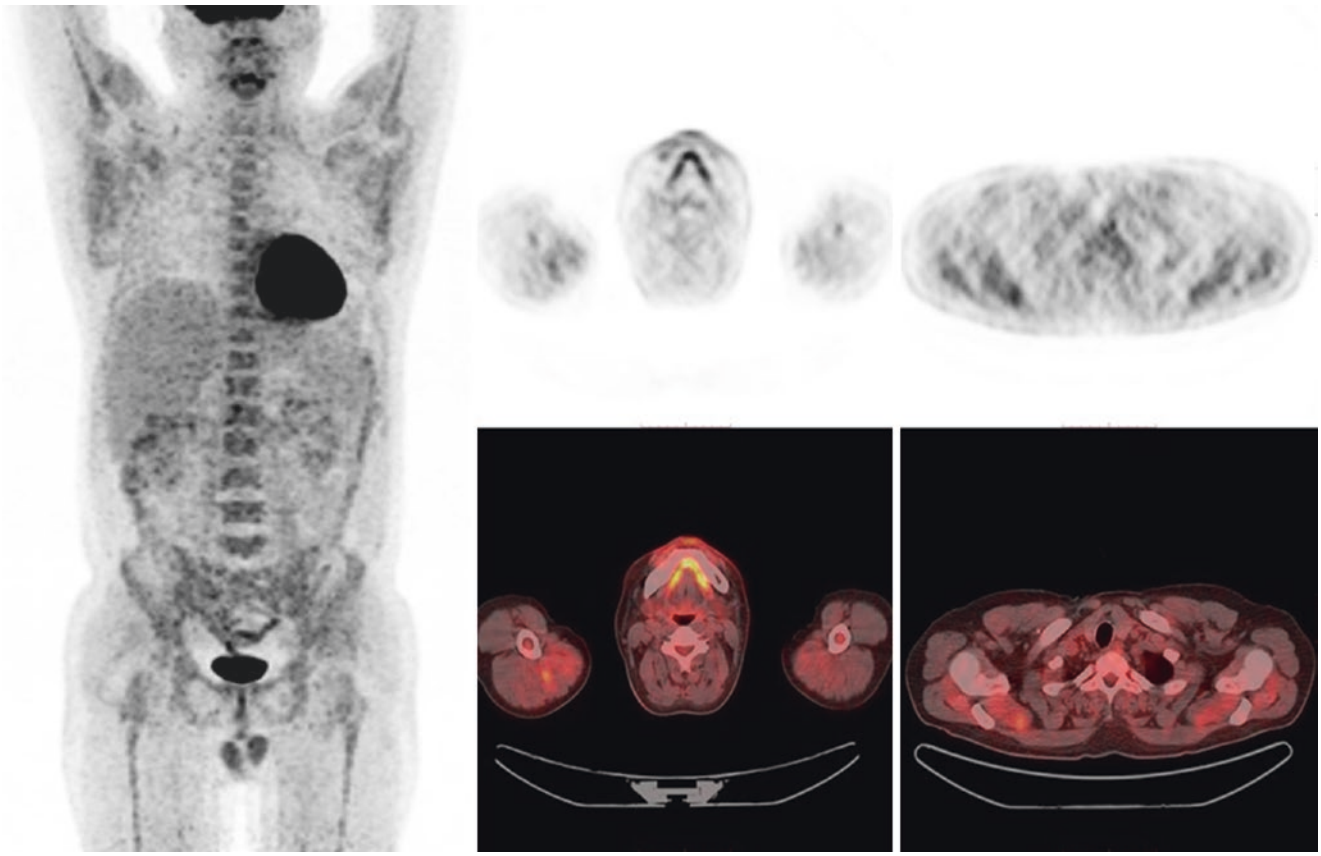

Fig. 6.2 Demonstrates moderate increased FDG uptake in PET/CT images in the whole body muscle, especially the bilateral upper limb muscles. In addition, systemic bone radioactivity uptake was significantly increased

6.3.3 Technique

- Patient preparation: the patient should not take anything by mouth for 6 h before administration of radiopharmaceutical.
- 460 MBq of 18FDG administered intravenously (body weight = 87 kg).
- Imaging device: whole body PET/CT camera (Siemens Biograph 64) with resolution of 4.0 mm FWHM.

6.3.4 Differential Diagnosis

- Infectious myopathy
- Metabolic myopathy
- Polymyalgia rheumatica
- Muscular dystrophy
- Tumor-associated myopathy

6.3.5 Diagnosis and Clinical Follow-Ups

This patient developed muscle aches and limb weakness in the limbs, and simultaneous hypokalemia. After receiving hormone combined with methotrexate therapy, the condition of the patient tended to be stable and is discharged from hospital.

6.3.6 Discussion

PM (polymyositis) and DM (dermatomyositis) are chronic inflammatory diseases that affect systemic skeletal muscles and extramuscular organs including the lungs [87, 88]. F18-FDG PET/CT has practicality and convenience in the clinical characterization of PM/DM [89, 90]. The biggest advantage of FDG PET is the fact that it can screen the entire body in one scan [91, 92].

6.4 Polymyositis

Xuena Li

Abstract Polymyositis is a disease with characteristic rash dominated by inflammation of skin and striated muscles. Skin and muscle damage can disappear or be mitigated after removal of tumors. An 18-year-old female developed lower limb weakness without inducement 6 months ago. Symptoms gradually worsened. The patient had difficulty swallowing in the past half-month, and occasionally coughed when drinking water. To exclude malignant tumors, the patient underwent PET/CT. Imaging showed multiple, symmetrical, and diffuse increased FDG uptake in head, neck, psoas major, and limb muscles, the viscera showed no lesion of increased metabolism. Muscle biopsy suggested myositis. Symptoms improved after hormone therapy.

Keywords: Polymyositis, FDG, PET

6.4.1 Clinical Presentation

An 18-year-old female developed lower limb weakness without obvious inducement 6 months ago, and her symptoms gradually worsened. The patient had difficulty swallowing in the past half-month, and occasionally had a cough when drinking water. Normal limb muscle tension. Head MRI prompted normal.

6.4.2 **Key Images** (Fig. 6.3)

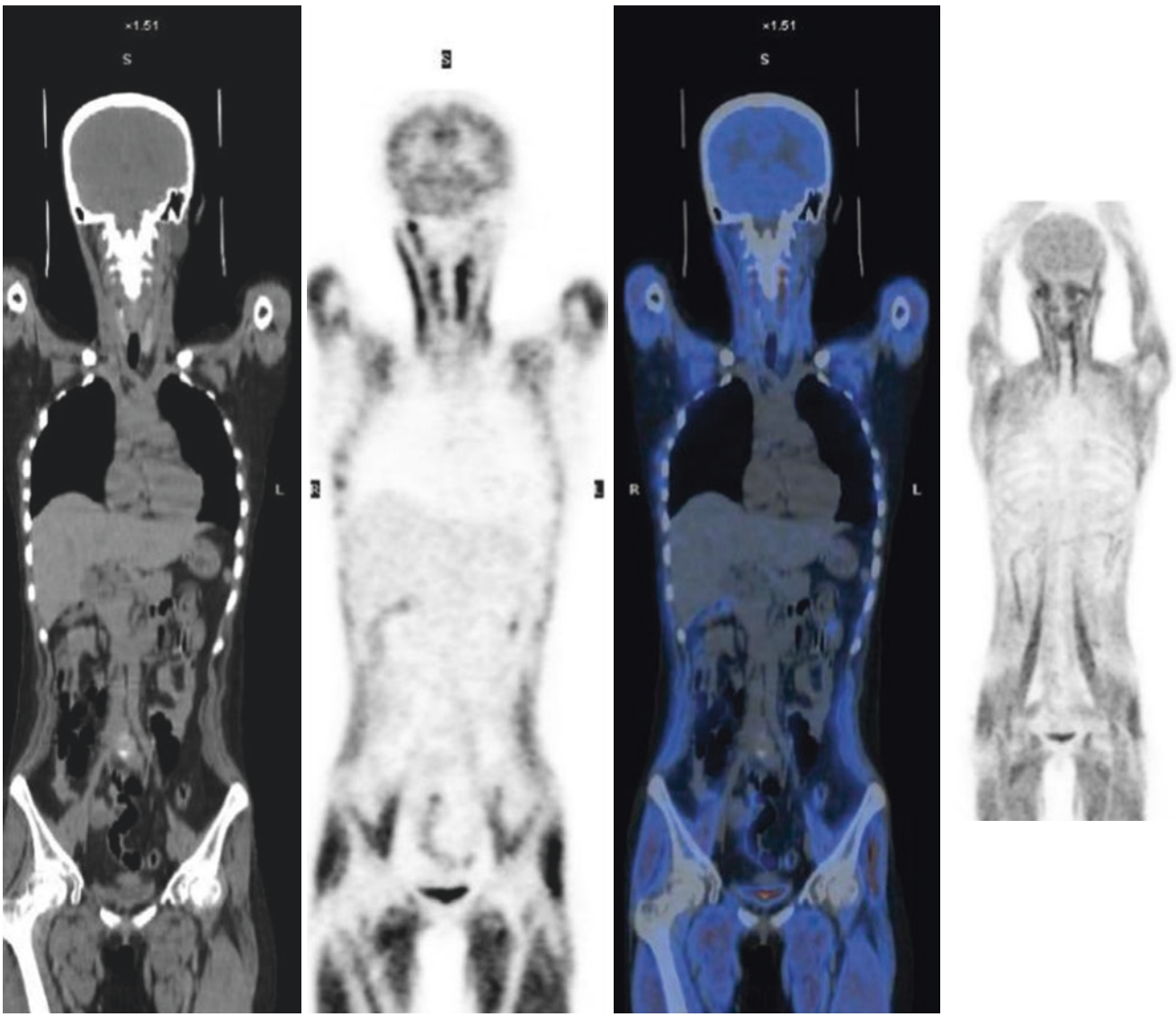

Fig. 6.3 ^{18}F-FDG PET/CT image

PET/CT imaging shows multiple, symmetrical, and diffuse increased FDG uptake in head, neck, psoas major, and limb muscles (SUV_{max} = 7.3), the viscera shows no lesions of increased metabolism

6.4.3 Technique

- Patient preparation: patient should not take anything by mouth for 6 h before administration of radiopharmaceutical.
- 185 MBq of 18F-FDG administered intravenously.
- Imaging device: whole body PET/CT camera (Siemens biograph) with resolution of 5.0 mm FWHM,

6.4.4 Differential Diagnosis

- Primary muscle tumor.
- Sarcoidosis.

6.4.5 Diagnosis and Clinical Follow-Ups

Muscle biopsy suggested myositis. The symptoms improved after the hormone therapy.

6.4.6 Discussion

Polymyositis is a disease with characteristic rash dominated by inflammation of skin and striated muscles. Inflammatory myopathy is a group of heterogeneous diseases. Malignant tumors are associated with polymyositis. Imaging contributes to exclude tumor-associated polymyositis [93, 94]. As a whole-body imaging, it shows lesions' distribution throughout the body and provides information for diagnosis [95, 96].

6.5 Dermatomyositis 1

Xuena Li

Abstract Polymyositis (PM) and dermatomyositis (DM) are idiopathic inflammatory myopathies that mainly involve skeletal muscles and other organs. Patients with DM present with characteristic skin lesions. A 65-year-old male was diagnosed with "systemic lupus erythematosus" 9 years ago, and his symptoms did not significantly improve after treatment with externally used drug. One month ago, the patient suffered from fatigue, facial edema, and rashes. Laboratory tests showed raisedd NSE. PET/CT imaging showed multiple elevated FDG uptake in the muscle with no primary tumors observed. The skin biopsy indicated DM.

Keywords: Dermatomyositis, FDG, PET

6.5.1 Clinical Presentation

A 65-year-old man was diagnosed with "systemic lupus erythematosus"9 years ago, and his symptoms did not significantly improved after external medication therapy. One month ago, the patient suffered from fatigue, facial edema, and rashes. Laboratory tests showed elevated NSE (30.47), serum levels of CK (128 U/L) and LDH (206 U/L).

6.5.2 Key Images

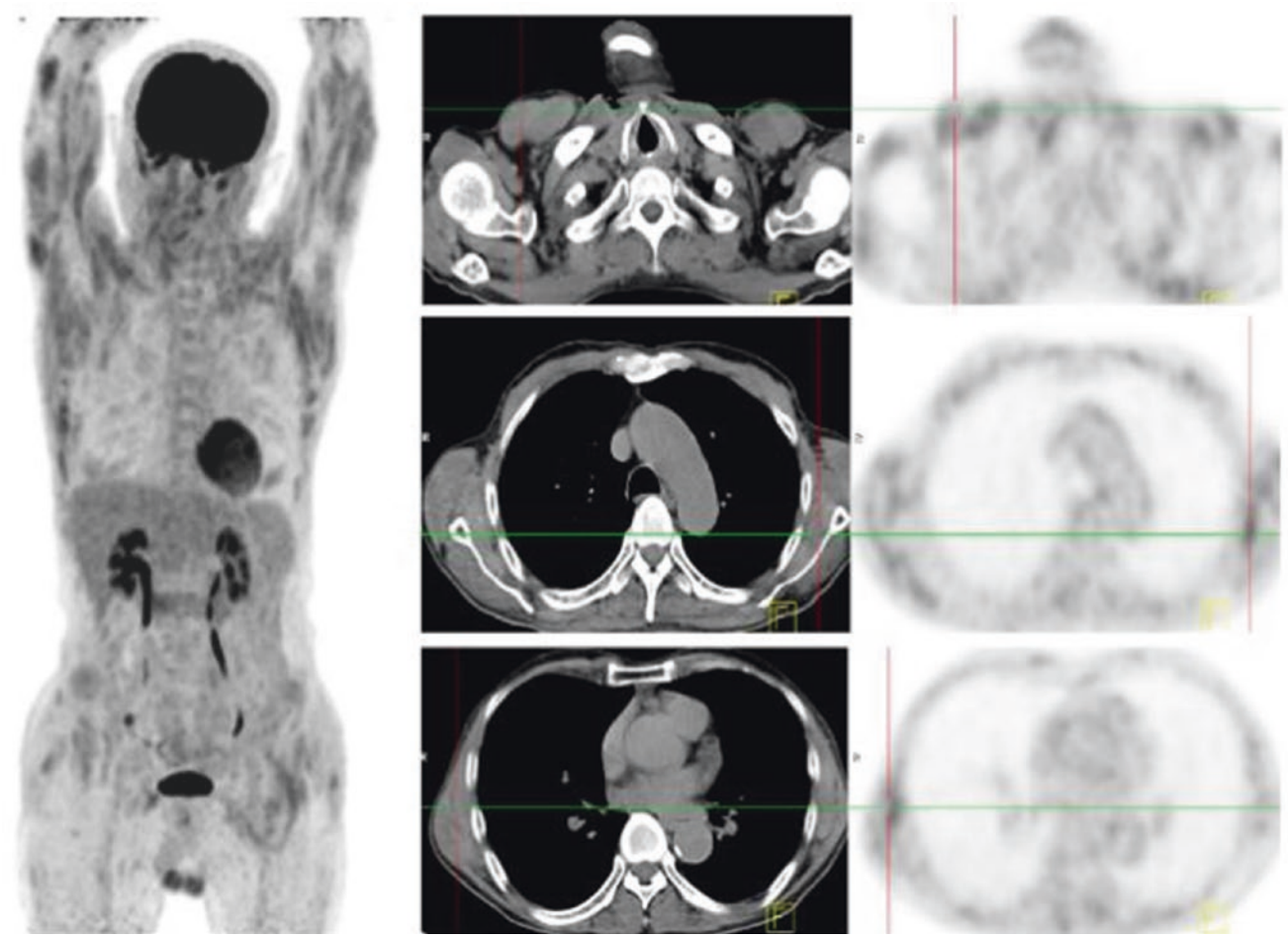

Fig. 6.4 ^{18}F-FDG PET/CT image

PET/CT imaging shows multiple elevated FDG uptake in the muscles without primary tumors

6.5.3 Technique

- Patient preparation: patient should not take anything by mouth for 6 h before administration of radiopharmaceutical.
- 185 MBq of 18F-FDG administered intravenously.
- Imaging device: whole body PET/CT camera (Siemens biograph) with resolution of 5.0 mm FWHM.

6.5.4 Differential Diagnosis

- Primary muscle tumor.
- Sarcoidosis.

6.5.5 Diagnosis and Clinical Follow-Ups

The skin pathology indicated dermatitis. The symptoms improved after specialist treatment.

6.5.6 Discussion

The diagnosis of DM is mainly based on the diagnostic and revised criteria proposed by Bohan and Peter in 1975. Some patients have no objective evidence of muscle inflammation. PET imaging has diagnostic value for DM and reflects disease activity by evaluating the metabolic activity of proximal band muscles [97–100].

6.6 Dermatomyositis 2

Azusa Tokue

Abstract Dermatomyositis (DM) is an idiopathic inflammatory myopathy characterized by skin rash and symmetric weakness of proximal muscles. We present a case of DM with FDG uptake in muscles assessed by PET/CT. The inflammatory lesions with increased FDG uptake were consistent with those of myositis detected by MRI. DM is often associated with malignancy and interstitial lung disease (ILD). FDG PET/CT may be useful for detection of malignancy and evaluation of active muscle inflammation, interstitial pneumonia in patients with DM.

Keywords: Dermatomyositis, FDG-PET/CT, Malignancy, Interstitial lung disease

6.6.1 Clinical Presentation

A 38-year-old woman presented with high fever, joint pain, and muscle pain for 2 months. She had heliotrope rash, Gottron's signs, mechanic's hands, and the weakness of proximal muscles. Muscle strength was evaluated by manual muscle test (MMT). Serum creatine kinase level was normal.

6.6.2 Key Images

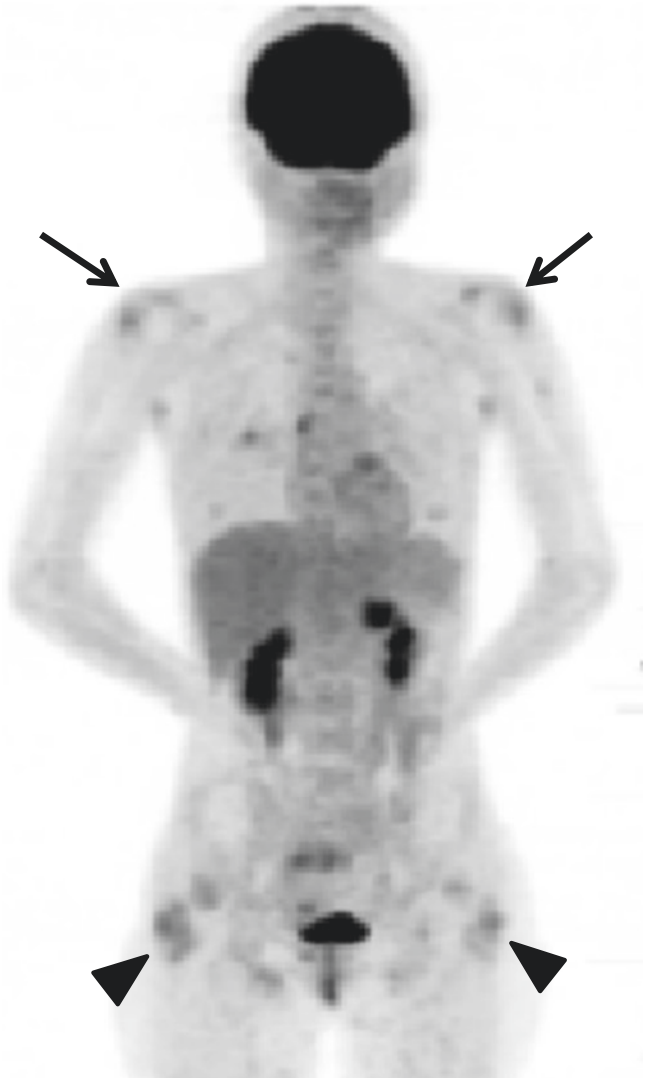

Fig. 6.5 MIP image showed multiple FDG uptakes in the bilateral deltoid muscles (arrow), bilateral gluteus maximus muscles (arrow head)

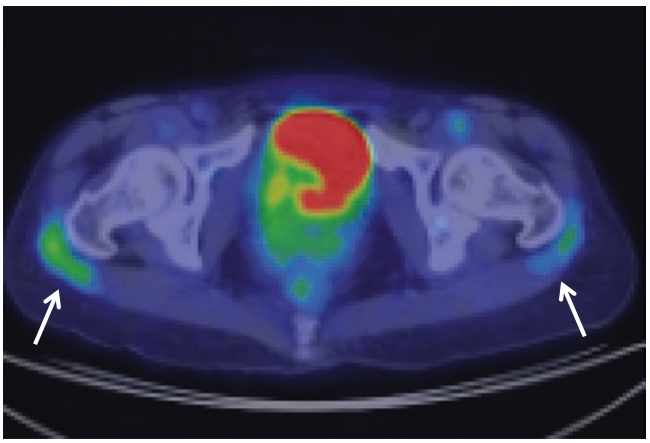

Fig. 6.6 PET/CT fusion image showed increased FDG uptakes in the bilateral gluteus maximus muscles (SUV_{max}: 2.1–2.8) (arrow)

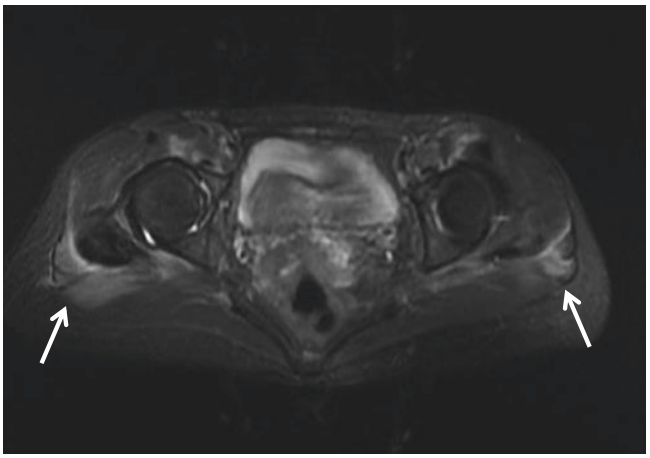

Fig. 6.7 Clinical diagnosis was DM. MRI scan demonstrated enhancement of bilateral gluteus maximus muscles consistent with FDG accumulation (arrow)

Fig. 6.8 CT showed reticular opacity in both lower lung and the complication of ILD was observed. She was treated with prednisolone, cyclophosphamide, and tacrolimus

6.6.3 Technique

- After fasting for at least 6 h, the patient was injected with FDG (5 MBq/kg) intravenously.
- PET/CT imaging was acquired 1 h after injection on a whole body PET/CT camera (Biograph 16, Siemens Medical Solutions) with resolution of 5.0 mm FWHM.
- MRI scan (Signa 1.5 T, GE) with a body total imaging matrix array coil was acquired.

6.6.4 Differential Diagnosis

- muscle strain,
- sarcoidosis.

6.6.5 Discussion

DM is a systemic autoimmune inflammatory myopathy with characteristic skin lesions and skeletal muscle inflammation [101]. Since DM patient often presents with malignancy and ILD [102], it is necessary to evaluate the distribution of whole body lesions before treatment. FDG PET/CT is useful for screening for malignancy, detecting inflammatory lesion of muscle and evaluating lung inflammation [103–105].

6.7 Rheumatoid Arthritis 1

Hiroyuki Yamashita

Abstract The main pathological manifestations of rheumatoid arthritis (RA) include synovitis, pannus formation and bone erosion. These pathological changes are usually assessed by plain X-ray, US, CT, and contrast-enhanced, fat-suppressed MRI. PET with 18F-FDG can be used to evaluate the metabolic activity of synovitis and measure the disease activity in RA patients by whole-body imaging. Imaging studies using 18F-FDG-PET have been performed to assess the metabolic activity of synovitis in patients with RA and to evaluate the disease activity of RA. Several reports have indicated that there was a significant correlation between the visual assessment of FDG uptake and clinical evaluation of disease activity.

Keywords: Rheumatoid arthritis, 18F-FDG-PET/CT, Disease activity

6.7.1 Clinical Presentation

An 86-year-old woman presented with polyarthritis. She had symmetrical polyarthritis that continued for more than 19 weeks with a severe inflammatory reaction (CRP, 12.72 mg/dL) and MRI findings that showed synovitis and tendinitis.

6.7.2 Key Images

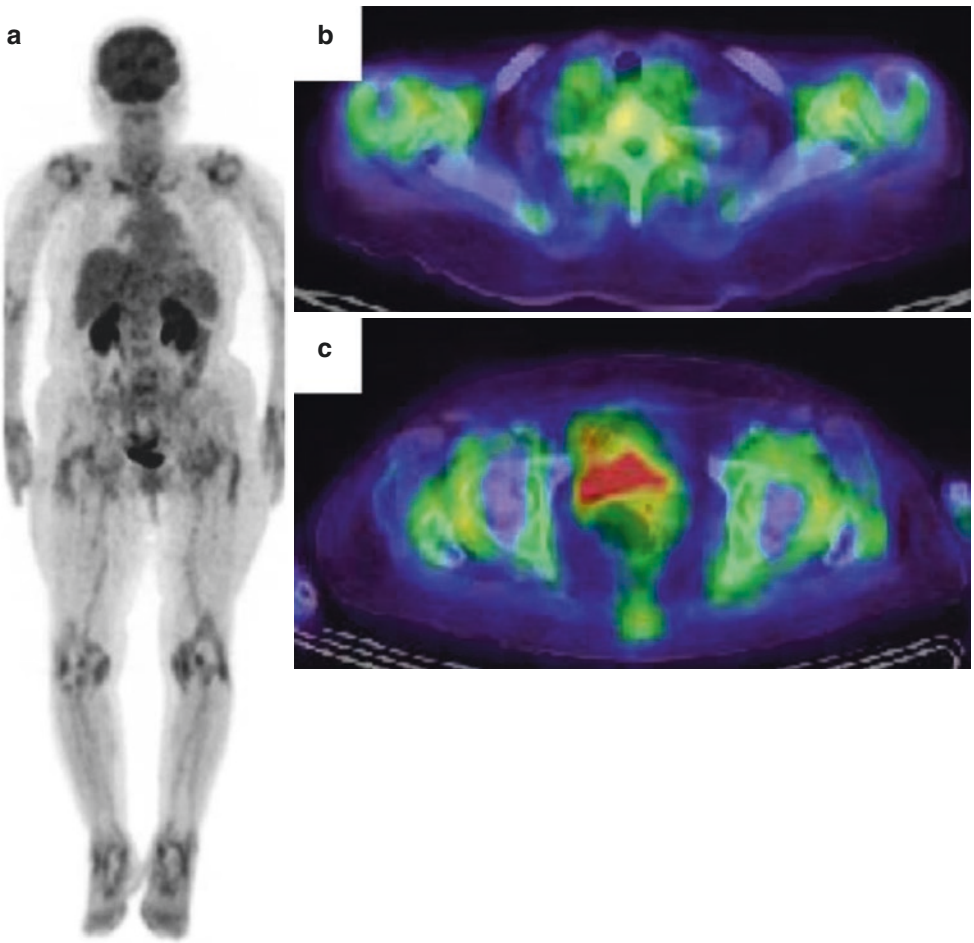

Fig. 6.9 (**a**–**c**) shows (**a**) MIP and (**b**, **c**) axial FDG-PET/CT findings. FDG-PET/CT showed (**a**) symmetrical arthritis and remarkable circular FDG uptake due to synovitis around the (**b**) shoulders and (**c**) hips.

6.7.3 Technique

- Patient preparation: The patient should not take anything orally up to 4 h before the administration of ^{18}FDG.
- 4–6 MBq/kg of ^{18}F-FDG was intravenously administered.
- Imaging device: Whole body PET/CT camera (Siemens biograph 16) with a resolution of 3.75 mm FWHM was used.

6.7.4 Differential Diagnosis

- Polymyalgia rheumatica (PMR)
- Spondyloarthritis (SpA)

6.7.5 Diagnosis and Clinical Follow-Ups

For this patient, clear synovitis was confirmed on MRI. Because polyarthritis in >11 sites and inflammatory reaction were observed, and the symptoms lasted for >6 weeks in spite of negative RF and anti-CCP antibody results, a diagnosis of RA was made based on the 2010 ACR/EULAR RA classification criteria.

6.7.6 Discussion

Active RA lesions were detected using ^{18}F-FDG PET/CT in our case. The disease activity of RA is determined through comprehensive examinations of the number of arthritis sites, degree of inflammatory reactions, and the degree of complaints from the patient. Occasionally, there is a discrepancy between the patient's complaints, inflammatory reactions, and the degree of arthritis upon physical examination. ^{18}F-FDG PET/CT is useful when comprehensively screening for latent arthritis and performing differential diagnoses of similar diseases, such as PMR and SpA [106–109].

6.8 Rheumatoid Arthritis 2

Xuena Li

Abstract Rheumatoid arthritis (RA) is a chronic autoimmune disorder with unknown etiology. The major clinical manifestations are chronic, symmetrical arthritis and extraarticular lesions. A 75-year-old male suffered from swelling and pain of the shoulders, knees, and hips without obvious inducement, accompanied by elevated blood NSE, underwent ^{18}F-FDG PET/CT for cancer screening. PET images showed increased FDG uptake of the bilateral shoulder joints, bilateral hip joints, gall bladder, and right cervical lymph nodes. Laboratory reports showed elevated C-reactive protein, erythrocyte sedimentation rate, and rheumatoid factor. The patient was diagnosed with rheumatoid arthritis and cholecystitis. After specialist treatment, his symptoms markedly improved.

Keywords: Rheumatoid arthritis, FDG, PET

6.8.1 Clinical Presentation

A 75-year-old man suffered from swelling and pain of the shoulders, knees, and hips with no apparent cause. The patient was diagnosed with gout by local hospital. The symptoms did not relieve after corresponding treatment. Ultrasonography indicated slightly higher echogenicity in the gall bladder. Laboratory reports showed elevated NSE.

6.8.2 Key Images

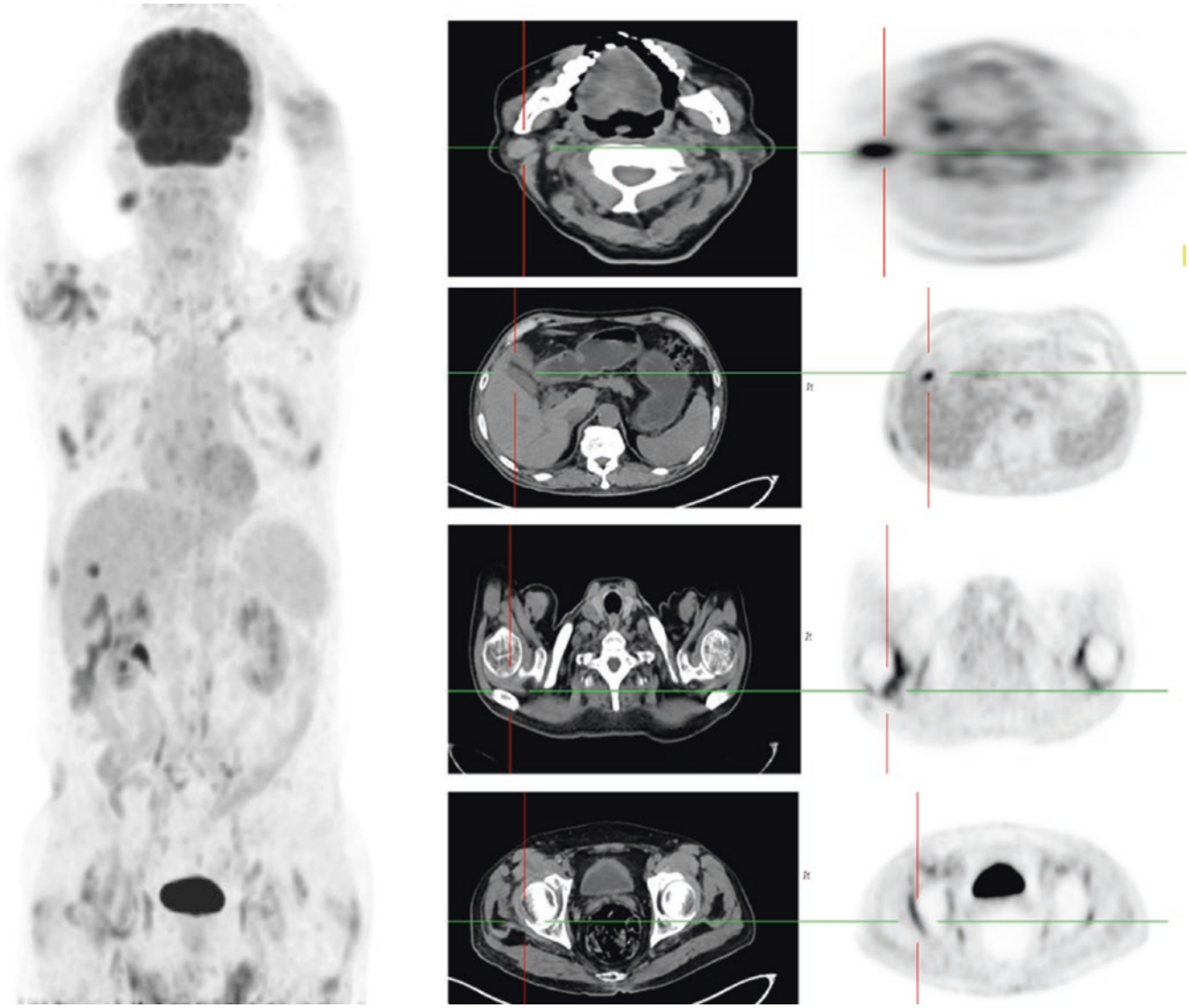

Fig. 6.10 ^{18}F-FDG PET/CT image

MIP image (Fig. 6.10) demonstrates increased tracer uptake in the bilateral shoulder joints, bilateral hip joints, gall bladder, and right cervical lymph nodes. Transverse image shows soft tissue in the bilateral shoulder joints and bilateral hip joints with increased FDG uptake

6.8.3 Technique

– Patient preparation: patient should not take anything by mouth for 6 h before administration of radiopharmaceutical.
– 185 MBq of 18F-FDG administered intravenously.
– Imaging device: whole body PET/CT camera (Siemens biograph) with resolution of 5.0 mm FWHM.

6.8.4 Differential Diagnosis

- Bone metastasis of malignant tumor.

6.8.5 Diagnosis and Clinical Follow-Ups

Laboratory reports showed elevated C-reactive protein, erythrocyte sedimentation rate, and rheumatoid factor. The patient was clinically diagnosed with rheumatoid arthritis. After specialist treatment, his symptoms markedly improved.

6.8.6 Discussion

FDG PET/CT has contributed to diagnosis and differential diagnosis of rheumatoid arthritis [110, 111]. This imaging always provides relatively objective overall information, helps to exclude malignant tumors and improves diagnostic accuracy [112]. ^{18}F-FDG PET/CT imaging can reflect activity and impact scope of rheumatoid arthritis, show more valuable information than conventional imaging modalities [113].

6.9 Polymyalgia Rheumatica

Hiroyuki Yamashita

Abstract Polymyalgia rheumatica (PMR) is a common disorder characterized by inflammatory pain and stiffness in the shoulder as well as in the pelvic girdle and neck. The diagnosis requires the exclusion of other conditions causing similar symptoms. Sometimes the complaints of PMR patients are vague and the diagnosis is difficult, based only on the chief complaints and the physical findings. FDG-PET/CT is useful for covering the entire body and identifying bursitis, a characteristic of PMR, which has vague symptoms and is difficult to identify from other imaging tests. As a result, FDG-PET/CT is useful for diagnosing PMR.

Keywords: Polymyalgia rheumatic, Bursitis, FDG-PET/CT

6.9.1 Clinical Presentation

The patient was a 58-year-old female whose chief complaint was an acute onset of neck pain and proximal myalgia. She exhibited an elevated inflammatory reaction (CRP level, 7.52 mg/dL; ESR, 104 mm/h), and an FDG-PET/CT scan was performed to investigate the cause. Blood culture test results were negative, and bacteremia was also negative.

6.9.2 **Key Images** (Fig. 6.11)

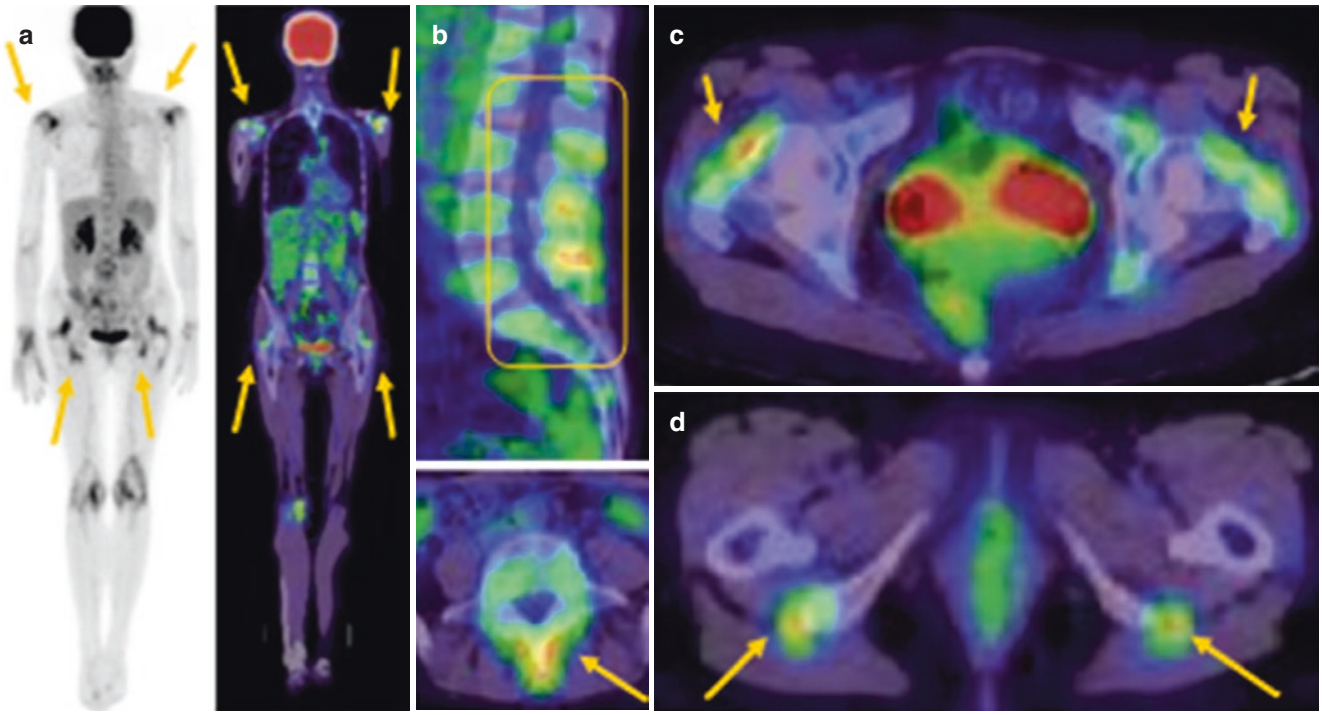

Fig. 6.11 (**a**, **b**) FDG-PET shows inflammatory FDG uptake in the shoulders and hips (arrows). Axial and sagittal FDG-PET/CT fusion images clearly show high FDG uptake in the intervertebral joints, interspinal ligaments, and surrounding muscles of the lumbar region (arrows) (**b**), and bursae in the greater trochanter (arrows) (**c**) and ischial tuberosity (arrows) (**d**)

6.9.3 Technique

- Patient preparation: patient should not take anything by mouth for 6 h before administration of radiopharmaceutical.
- -185 MBq of 18FDG administered intravenously.
- Imaging device: whole body PET/CT camera (Siemens biograph) with resolution of 5.0 mm FWHM.

6.9.4 Differential Diagnosis

- Rheumatoid arthritis (RA).
- Spondyloarthritis (SpA).

6.9.5 Diagnosis and Clinical Follow-Ups (Fig. 6.12)

6.9.6 Discussion

Active RA lesions were detected using ^{18}F-FDG PET/CT in our case. PMR patients showed increased FDG uptake in ischial tuberosities, greater trochanters, and lumbar spinous processes [114]. Positive results at two or more of these sites showed high sensitivity and specificity for the diagnosis of PMR. Moreover, the pattern of accumulation in the shoulder (focal and nonlinear uptake patterns) and the identification of iliopectineal bursitis are useful in diagnosing PMR, which is at times difficult to differentiate from elderly-onsetRA [109, 115].

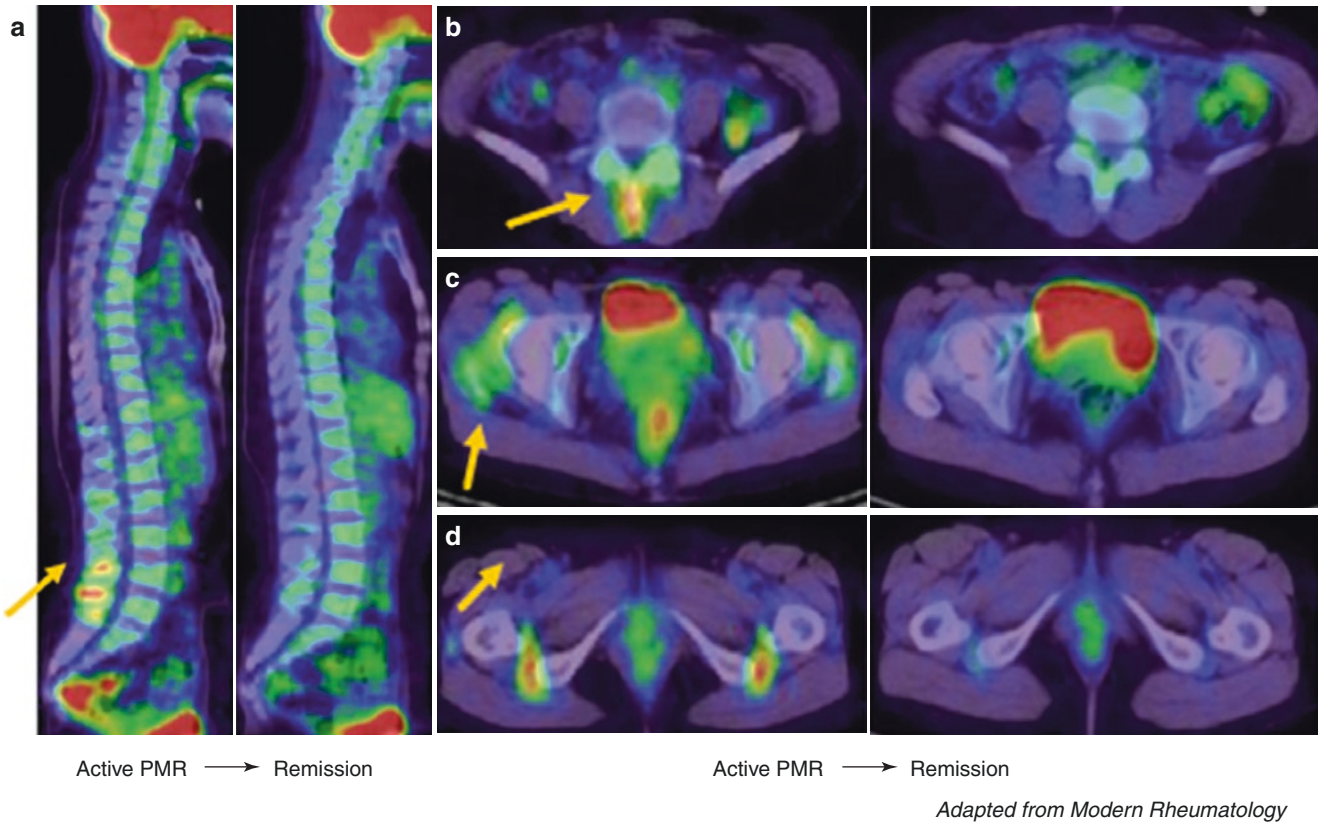

Fig. 6.12 Because the patient was ≥50 years, her ESR was ≥40 mm/h; further, she had proximal myalgia and experienced a prompt therapeutic reaction to steroids. She was evaluated as having met the Chuang et al. and Healy criteria, which led to a diagnosis of PMR. A follow-up FDG-PET/CT shows that FDG uptake in the spinous processes of the lower lumbar vertebrae (**a**, **b**, arrows), greater trochanter (**c**, arrows), and ischial tuberosity (**d**, arrows) normalized after therapy (**a**–**d**, right panels)

6.10 Relapsing Polycondritis

Hiroyuki Yamashita

Abstract Relapsing polychondritis (RPC) is a rare multisystemic disease characterized by recurrent inflammation of the cartilaginous structures of the external ear, nose, peripheral joints, larynx, and tracheobronchial tree. Much remains unknown about the epidemiology of RPC. Diagnosis is made according to the empirically defined clinical criteria of McAdam et al. No specific histological finding is considered pathognomonic for this disease. FDG-PET/CT may be a powerful tool for the early diagnosis of relapsing polychondritis, especially when patients have no involvement of organs that are easily biopsied such as the ears or nose. It is also useful for determining the extent of disease and monitoring disease activity during treatment.

Keywords: Relapsing polychondritis, FDG-PET/CT

6.10.1 Clinical Presentation

A 74-year-old female presented with nasal symptoms. She was positive for type II anti-collagen antibody, and nasal cartilage biopsy findings were consistent with RPC.

6.10.2 Key Images (Fig. 6.13)

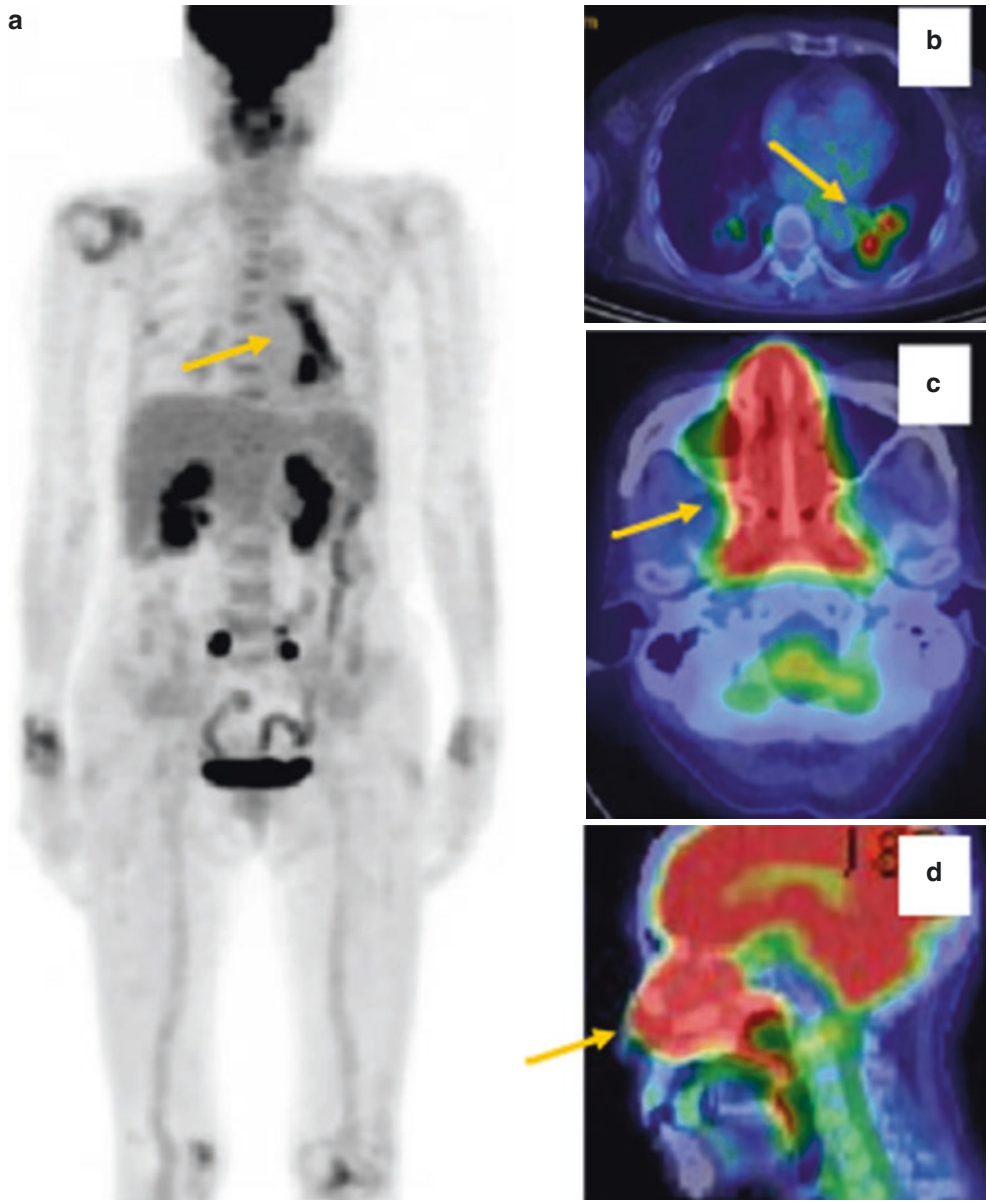

Fig. 6.13 Well-defined FDG accumulations (SUV_{max}: 13.03) in the area extending from the infrahilar region of the left inferior lobe to the pulmonary hilus are noted (**a**, **b**, *arrow*). There was no radiographic evidence of bronchial wall thickening or bronchial stricture. Conspicuous FDG accumulation (SUV_{max}: 9.50) was also noted in the nasal cavity (**c**, **d**, *arrow*)

6.10.3 Technique

- Patient preparation: patient should not take anything by mouth for 6 h before administration of radiopharmaceutical.
- 185 MBq of 18FDG administered intravenously.
- Imaging device: whole body PET/CT camera (Siemens biograph) with resolution of 5.0 mm FWHM.

6.10.4 Differential Diagnosis

- Infection or malignancy
- Chondrodermatitis nodularis helicis
- Red ear syndrome Epiglottitis Rhinoscleroma Pemphigus vulgaris
- Mediastinal lesions affecting the tracheal wall
- Granulomatosis with polyangiitis
- Systemic inflammatory polyarthritis
- Aortitis and aortic aneurysms

6.10.5 Diagnosis and Clinical Follow-Ups (Fig. 6.14)

Based on the diagnostic criteria established by Damiani et al., the definitive diagnosis was RPC, because nasal chondritis and associated histological findings were confirmed.

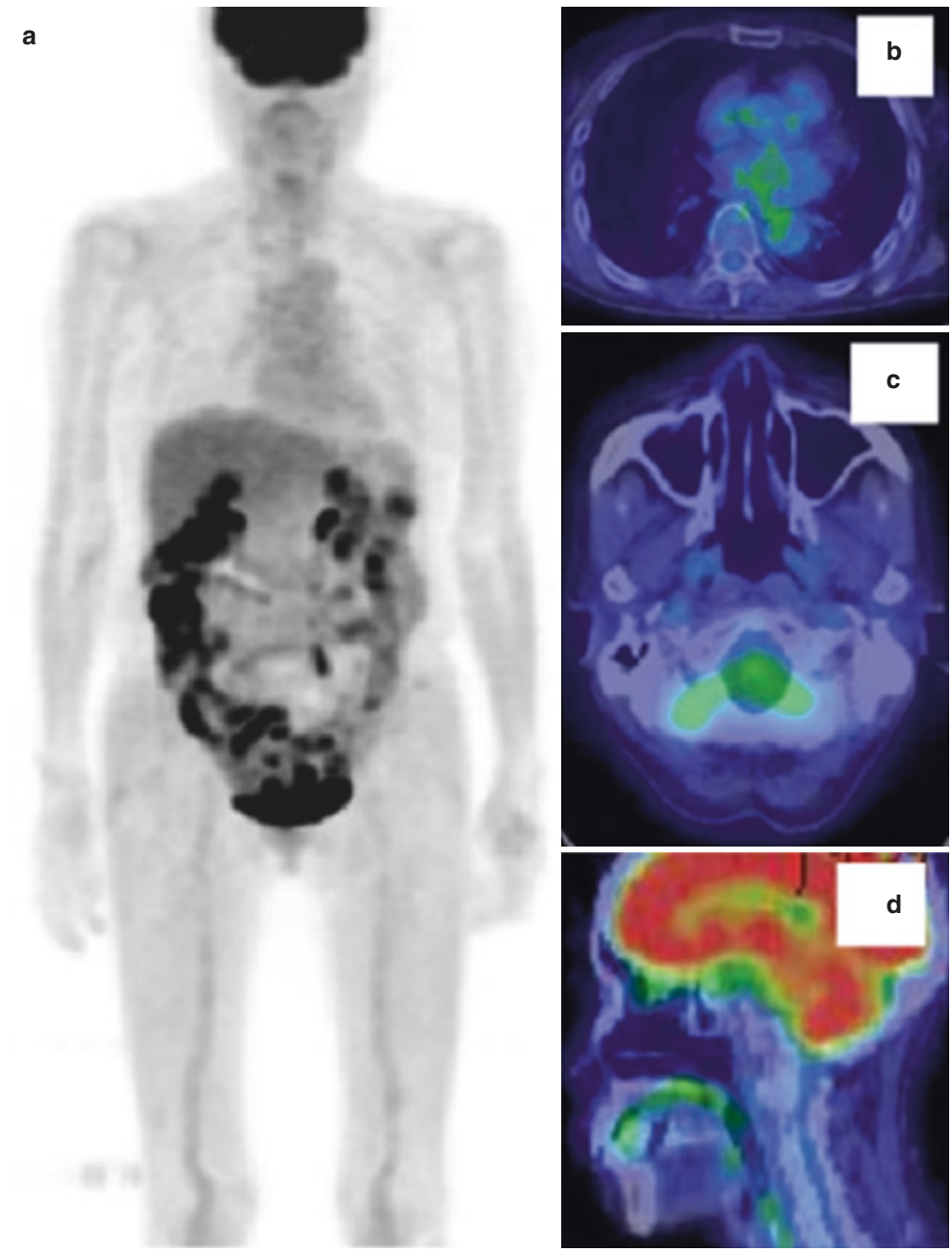

Fig. 6.14 (**a**, **b**) Posttreatment FDG PET/CT images showed complete lack of FDG accumulation in the area extending from the infrahilar region of the left inferior lobe to the pulmonary hilus. (**c**, **d**) Conspicuous FDG accumulation in the nasal cavity disappeared completely after treatment

6.10.6 Discussion

FDG-PET/CT is a potentially powerful tool for the early diagnosis of RPC, especially in patients without easily biopsied organ involvement [109, 116, 117]. This modality also facilitates the evaluation of extent of disease and disease activity during treatment. In addition, FDG-PET/CT guides biopsy site by identifying the active inflammation of asymptomatic lesions in relapsing polychondritis.

6.11 Granulomatosis with Polyangiitis 1

Xuena Li

Abstract Granulomatosis with polyangiitis (GPA) is complex, various and lack of specificity in clinical manifestations. The most commonly involved organs and systems are ears, nose, throat, lungs, and kidneys. A 56-year-old male appeared with epistaxis, discharging pus, and smelly secretions 6 months ago. It was considered sinusitis. In the past 2 months, instep skin and the sacrococcygeal region ulcerated and formed scabs. PET imaging was used to exclude malignant tumors. PET/CT showed soft tissue density shadow in bilateral maxillary sinus and nasal cavity, FDG uptake increased uneven. Metabolism in spleen and bone marrow increased diffusely. Laboratory tests showed positive ANCA. Symptoms relieved after hormone therapy.

Keywords: Granulomatosis with polyangiitis, FDG, PET

6.11.1 Clinical Presentation

A 56-year-old male appeared with epistaxis, discharging pus, and smelly secretions 6 months ago. It was considered sinusitis. Anti-inflammatory treatment is not effective. In the past 2 months, instep skin and sacrococcygeal region ulcerated and formed scabs. He had pain in lower limbs with swelling feet and difficulty in walking. CA12-5 and CRP increased (Fig. 6.15).

Key Images PET/CT imaging shows soft tissue density shadow in the bilateral maxillary sinus and nasal cavity, the FDG uptake increases uneven (SUV_{max} = 8.7), the metabolism in the spleen and bone marrow in visual field increases diffusely (SUV_{max} = 5.1)

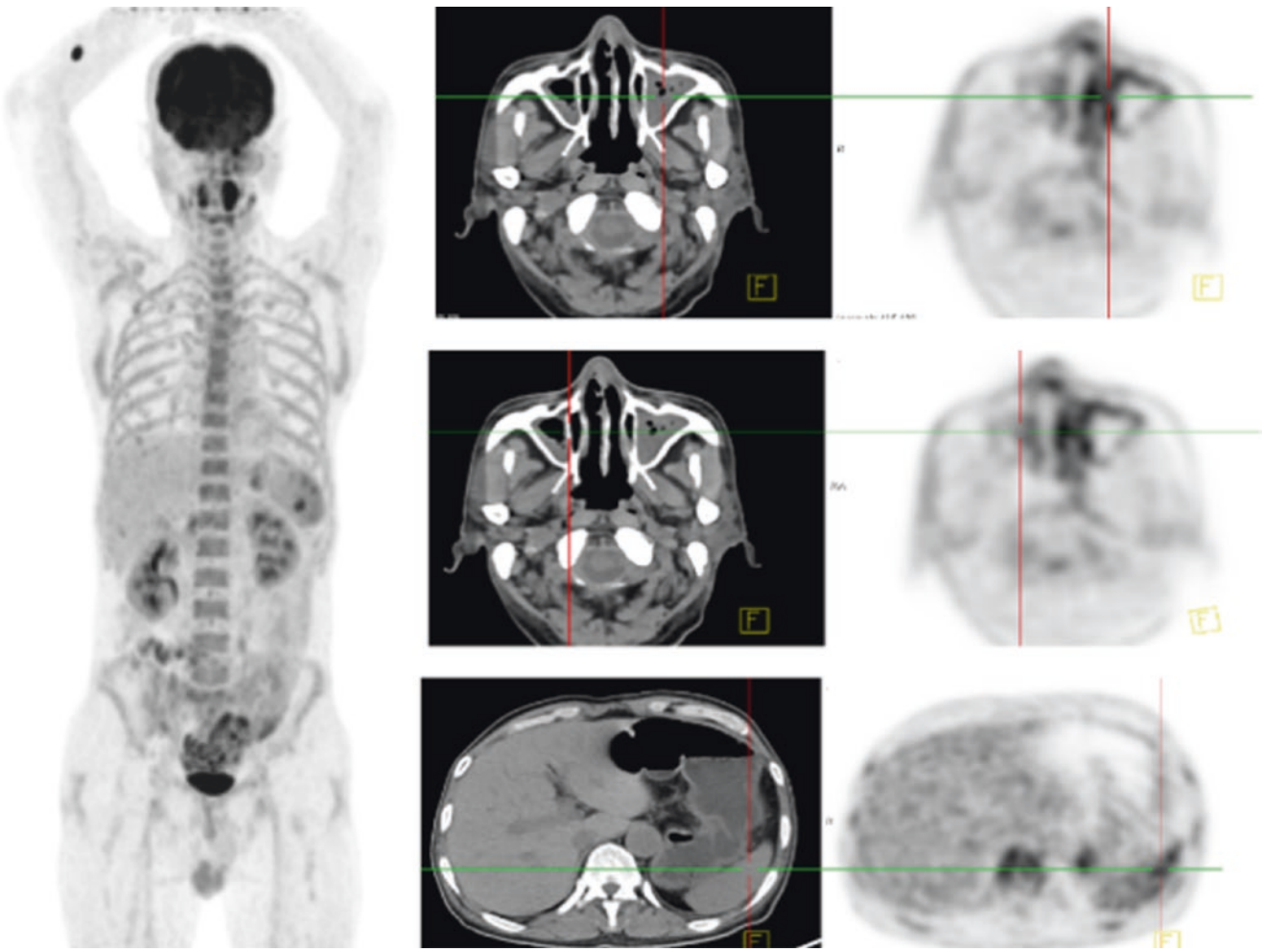

Fig. 6.15 ^{18}F-FDG PET/CT image

6.11.2 Technique

- Patient preparation: patient should not take anything by mouth for 6 h before administration of radiopharmaceutical.
- 185 MBq of 18F-FDG administered intravenously.
- Imaging device: whole body PET/CT camera (Siemens biograph) with resolution of 5.0 mm FWHM,

6.11.3 Differential Diagnosis

- Primary muscle tumor.
- Sarcoidosis.

6.11.4 Diagnosis and Clinical Follow-Ups

Bone marrow puncture showed reactive hyperplasia. After hormone therapy, the symptoms relieved significantly.

6.11.5 Discussion

Granulomatosis with polyangiitis (GPA) involves nasopharynx, so it is easy to be misdiagnosed. PET/CT is positive in GPA and used as an auxiliary diagnostic method to assess extent of lesions and range of systemic involvement [118, 119]. PET/CT positive lesions need to be confirmed by pathology and follow-up after treatment [120, 121].

6.12 Granulomatosis with Polyangiitis 2

Kimiteru Ito

Abstract Granulomatosis with polyangiitis (GPA), also known as Wegener's granulomatosis, is a rare disease characterized by granulomatous necrotizing vasculitis, which primarily involves small- and medium-sized blood vessels. GPA is a rare type of systemic vasculitis that involves the upper and lower respiratory tracts and the kidneys. Severe inflammation and renal failure rapidly develops in untreated patients and can be life-threatening. Therefore, early diagnosis is essential to improve prognosis. A considerably high ^{18}F-FDG uptake is exhibited in GPA before treatment; however, the uptake promptly decreases after treatment. In this study, ^{18}F-FDG PET/CT was used in the diagnosis and follow-up of patients with GPA.

Keywords: Granulomatosis with polyangiitis, Wegener's granuloma, Vasculitis, ANCA, PET/CT

6.12.1 Clinical Presentation

A 79-year-old woman with fever of unknown origin underwent ^{18}F-FDG PET/CT. Chest X-ray showed that both lung lesions resisted antibiotic therapy. Laboratory findings showed that serum MPO-circulating antineutrophil cytoplasmic antibodies (ANCAs) titer was elevated, whereas serum PR3–ANCA titer was within the normal limits.

6.12.2 Key Images (Fig. 6.16–6.19)

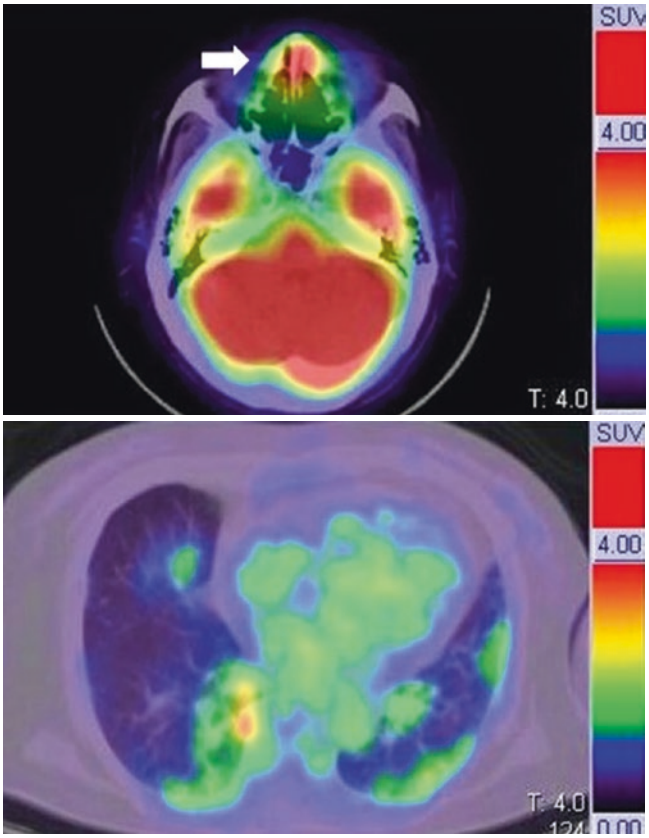

Fig. 6.16 Axial ^{18}F-FDG PET/CT showed abnormal ^{18}F-FDG uptake in the nasal wall (white arrow; SUV_{max}, 5.1). Axial ^{18}F-FDG PET/CT showed increased ^{18}F-FDG uptake in the opacities in both lungs (SUV_{max}, 4.0) in this figure.

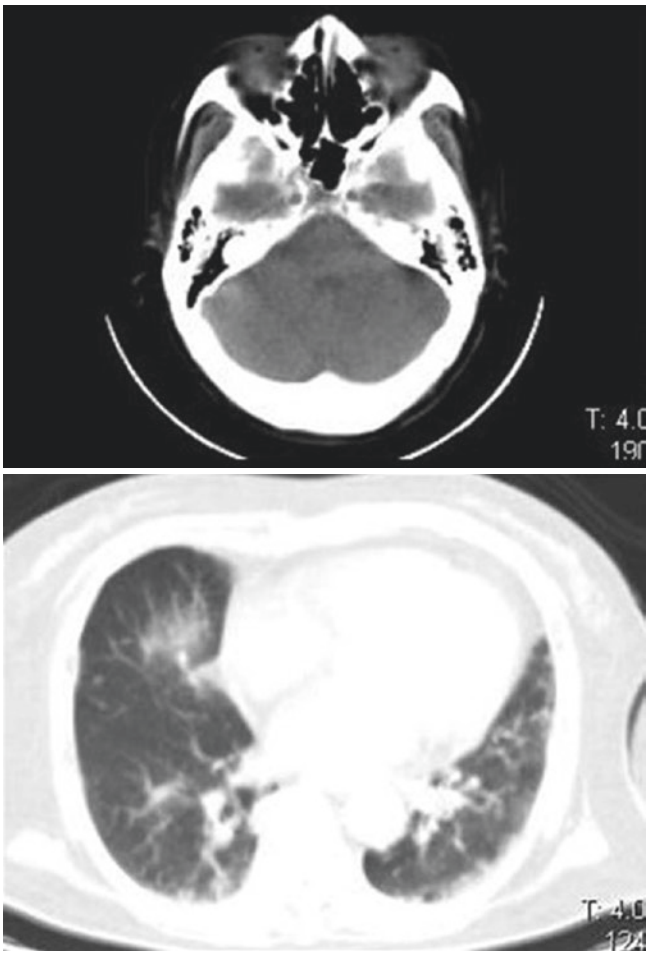

Fig. 6.17 Nonenhanced CT alone did not show the nasal lesion in this figure

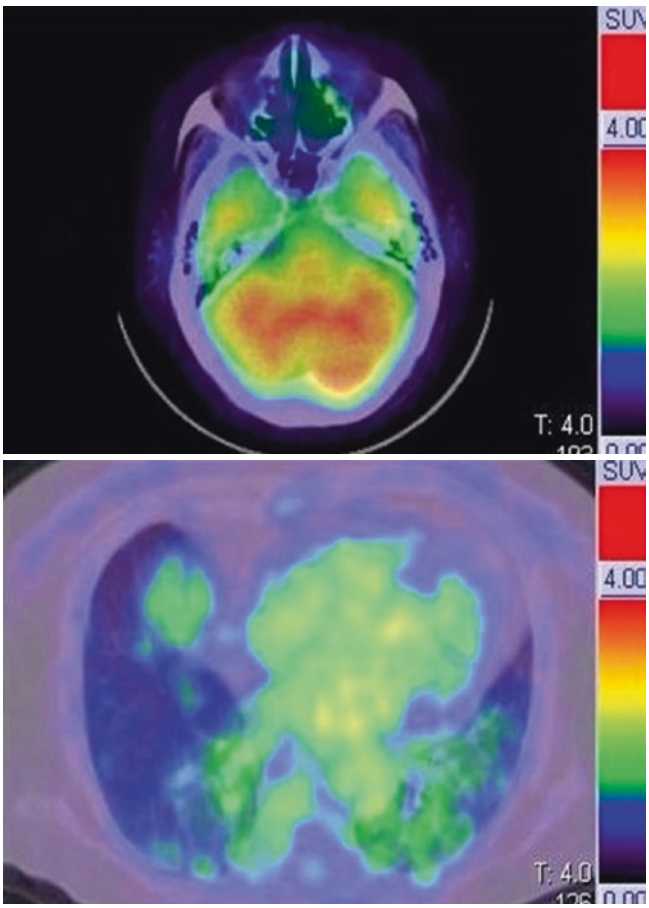

Fig. 6.18 The patient was diagnosed with GPA using nasal biopsy from ^{18}F-FDG uptake area. A follow-up ^{18}F-FDG PET/CT in this figure showed no ^{18}F-FDG uptake in the nasal mucosa after the administration of prednisolone and immunosuppressant therapy

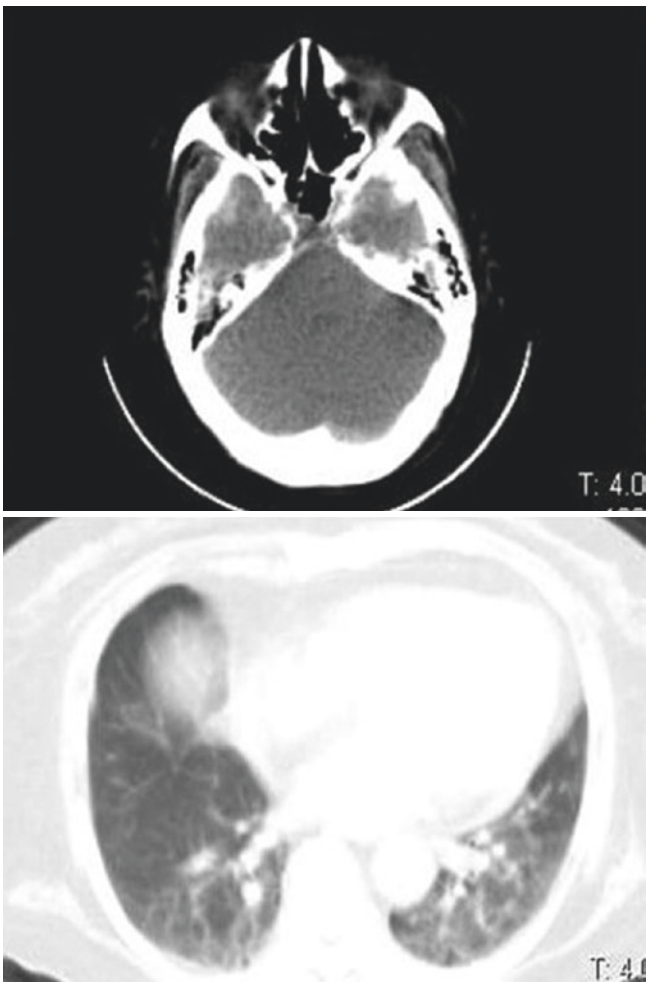

Fig. 6.19 ^{18}F-FDG uptake in the opacities in both lungs decreased

6.12.3 Technique

- Patient preparation: The patient should not take anything orally up to 4 h before the administration of ^{18}FDG.
- 4–6 MBq/kg of ^{18}F-FDG was intravenously administered.
- Imaging device: Whole body PET/CT camera (Siemens biograph 16) with a resolution of 3.75 mm FWHM was used.

6.12.4 Differential Diagnosis

- Various malignancies (for example, lymphoma and lung cancer)
- Sarcoidosis
- Mycobacterium
- Other collagen diseases

6.12.5 Discussion

Active GPA lesions were detected using ^{18}F-FDG PET/CT in our case. GPA lesions in the upper respiratory tract were easier to detect using ^{18}F-FDG PET/CT than using nonenhanced CT alone [122–125]. Notably, all radiologists must be familiar with the clinical features and ^{18}F-FDG PET of GPA.

6.13 Systemic Lupus Erythematosus

Xuena Li

Abstract Systemic lupus erythematosus (SLE) is an autoimmune connective tissue disease involving organs and systems. A 35-year-old female appeared with lumbago without incentives. Main clinical symptoms were bilateral renal pain, bilateral elbows, shoulders and knees pain, stiffness, and

fever. Laboratory tests showed positive antinuclear antibody, anti-Smith, anti-U1RNP, and increased immunoglobulin IgG, CK, and LDH. PET/CT showed increased FDG uptake in lymph nodes in bilateral cervical, supraclavicular, inguinal, mediastinal, retroperitoneal, and left axillary regions, some of which were enlarged, diffusely elevated uptake in spleen and patchy increased-density shadow in both lungs with uneven rising metabolism. Symptoms improved by hormone, cyclophosphamide, and immunomodulatory therapy.

Keywords: Systemic lupus erythematosus, FDG, PET

6.13.1 Clinical Presentation

A 35-year-old female appeared with lumbago without obvious incentives. The main clinical symptoms were bilateral renal pain, bilateral elbows, shoulders and knees pain, stiffness, and fever. Laboratory tests showed positive antinuclear antibody (ANA), anti-Smith, anti-U1RNP, and increased immunoglobulin IgG, CK, and LDH.

6.13.2 Key Images

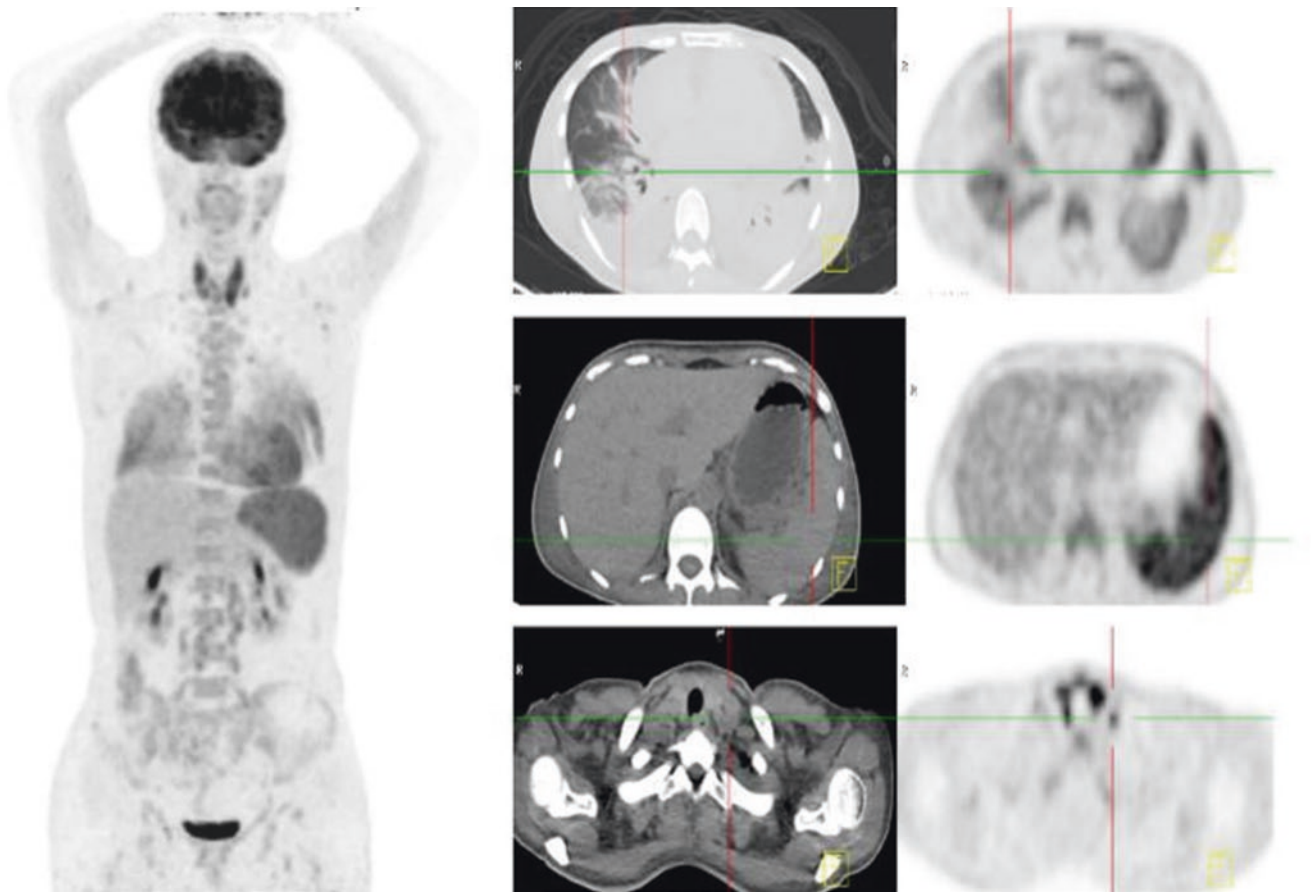

Fig. 6.20 ^{18}F-FDG PET/CT image

PET/CT shows increased FDG uptake in lymph nodes in bilateral cervical, supraclavicular, inguinal, mediastinal, retroperitoneal, and left axillary regions, some of which are enlarged, diffusely elevated uptake in spleen and patchy increased-density shadow in both lungs with uneven rising metabolism

6.13.3 Technique

- Patient preparation: patient should not take anything by mouth for 6 h before administration of radiopharmaceutical.
- 185 MBq of 18F-FDG administered intravenously.
- Imaging device: whole body PET/CT camera (Siemens biograph) with resolution of 5.0 mm FWHM,

6.13.4 Differential Diagnosis

- Primary muscle tumor
- Sarcoidosis

6.13.5 Diagnosis and Clinical Follow-Ups

The symptoms improved after hormone, cyclophosphamide, and immunomodulatory therapy.

6.13.6 Discussion

SLE is an autoimmune connective tissue disease involving multiple organs. Chest is often involved because it is rich in connective tissue. The early diagnosis of SLE is vital for its clinically acute onset, rapid progress, and high mortality. PET/CT of pulmonary lesions can present positive changes that reflect disease activity [126–128].

6.14 IgG4-Related Diseases; Autoimmune Pancreatitis and Lymphadenitis

Kazuhiro Oguchi

Case 1. Abstract An 80-year-old man received FDG-PET/CT for preoperative staging of gastric cancer. PET/CT images showed diffuse pancreatic FDG uptake as well as abnormal uptake into the bilateral supraclavicular, mediastinal, hilar, and abdominal lymph nodes and retroperitoneal soft tissue. His serum IgG4 was elevated. Pathological examination of a gastro-duodenal specimen revealed infiltration of numerous IgG4-positive plasma cells to confirm a diagnosis of IgG4-related disease. Diffuse or multifocal pancreatic FDG uptake is a characteristic finding of IgG4-related autoimmune pancreatitis. Extra-pancreatic uptake in specific organs is also helpful to identify IgG4-related disease.

Keywords: Autoimmune pancreatitis, IgG4-related disease, lymphadenopathy

6.14.1 Clinical Presentation

An 80-year-old man complained of abdominal pain. CT images revealed swelling of the pancreas. Blood testing showed slight elevation of serum IgG4. Ten months later, he underwent FDG-PET/CT for preoperative staging of gastric cancer. His serum IgG4 was elevated at 873 mg/dL.

6.14.2 Key Images (Fig. 6.21)

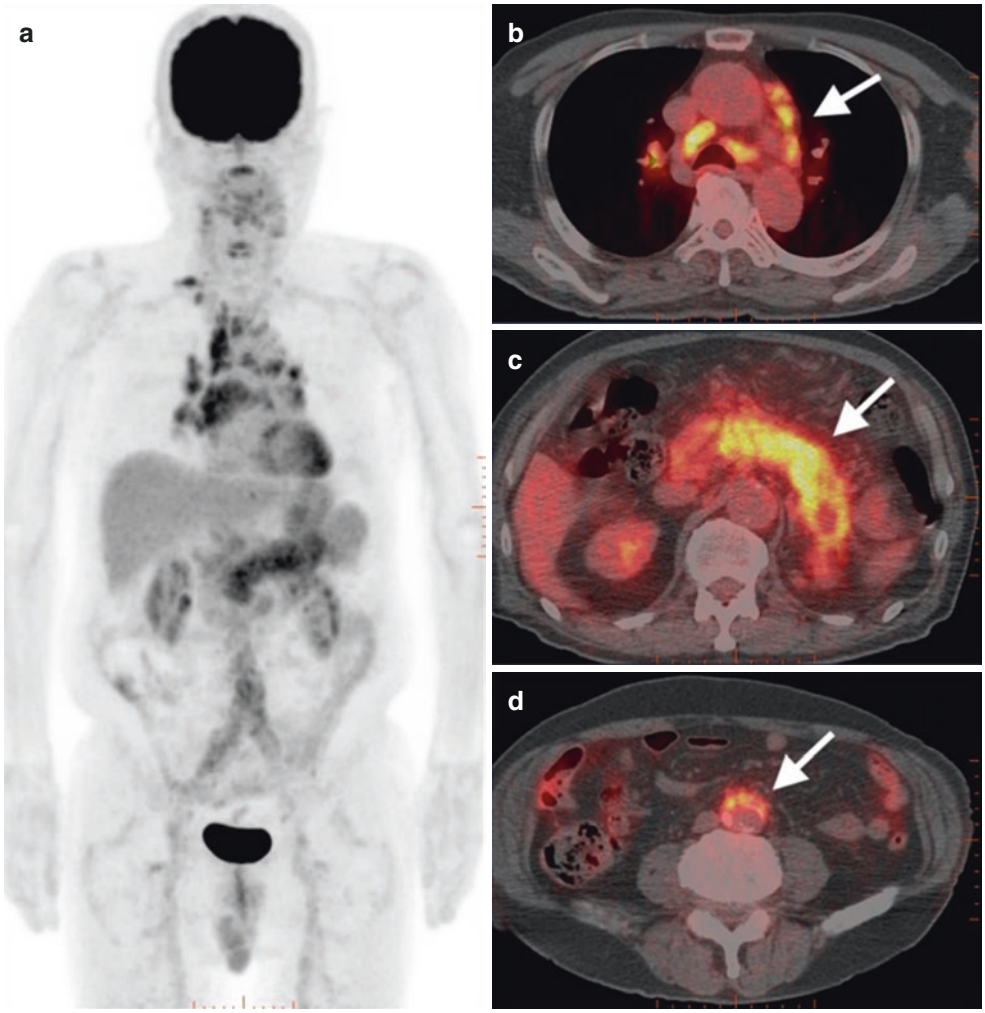

Fig. 6.21 Case 1 ^{18}F-FDG PET/CT

6.14.3 Technique

The patient fasted for over 5 h before PET examination.

A total of 264 MBq (4 MBq/kg) of F-18 FDG was administrated intravenously.

Whole-body PET/CT images were obtained using a PET/CT scanner (Discovery PET/CT 600, GE) with a spatial resolution of 5.1 mm FWHM at 60 min after FDG injection.

6.14.4 Image Interpretation

A swollen pancreas and diffuse FDG uptake were seen (c). Bilateral supraclavicular, mediastinal (b), and hilar lymph nodes displayed swelling and increased FDG uptake. Abnormal FDG uptake in the abdominal lymph nodes and retroperitoneal soft tissue (d) were also evident.

6.14.5 Differential Diagnosis

IgG4-related disease, malignant lymphoma, pancreatic cancer with metastases, sarcoidosis, multicentric Castleman disease.

6.14.6 Diagnosis and Clinical Follow-Up

The patient received surgery for gastric cancer. Pathological examination confirmed the infiltration of IgG4-positive plasma cells in the duodenum and pyloric walls, which met the diagnostic criteria for IgG4-related disease.

6.14.7 Discussion

Diffuse or multifocal pancreatic FDG uptake is a hallmark of IgG4-related autoimmune pancreatitis [129]. Extrapancreatic uptake in the submandibular gland, mediastinal and hilar lymph nodes, and retroperitoneal soft tissue are also helpful to diagnose IgG4-related disease [129–131]. Abnormal uptake in many other organs, including the pituitary gland, cranial nerve, biliary tract, kidney, and prostate gland, has been reported in patients with IgG4-related disease [131, 132].

Case 2. Abstract A 78-year-old man was referred to an institution for anemia and renal dysfunction. FDG-PET/CT showed abnormal FDG uptake in the pancreas, salivary glands, systemic lymph nodes, para-aortic soft tissue, prostate gland, and kidneys. IgG4-related disease was diagnosed after pathological examination of a renal biopsy revealed IgG4-related tubulointerstitial nephritis. Special attention should be paid for abnormal uptake of FDG in the cortical region of the kidney or prostate gland.

Keywords: Autoimmune pancreatitis, IgG4-related disease, lymphadenopathy, Renal FDG uptake

6.14.8 Clinical Presentation

A 78-year-old man under treatment for diabetes mellitus was referred to a hospital for examination of anemia. CT images revealed swelling of the pancreas, liver, spleen, and bilateral kidneys. Serological testing showed IgG4 elevation (420 mg/dL) and renal dysfunction.

6.14.9 **Key Images** (Fig. 6.22)

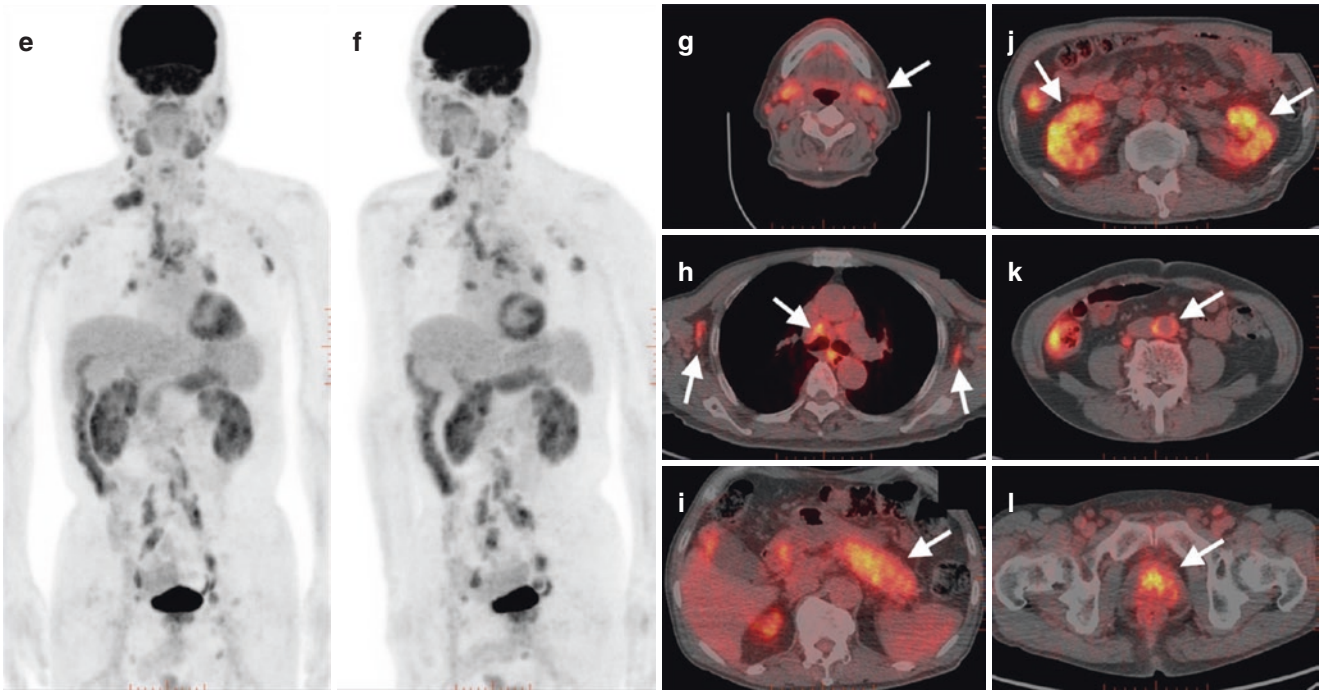

Fig. 6.22 Case 2 ^{18}F-FDG PET/CT

6.14.10 Technique

The patient fasted for over 5 h prior to PET examination.

A total of 249 MBq (4 MBq/kg) of F-18 FDG was administrated intravenously.

Whole-body PET/CT images were obtained using a PET/CT camera (Discovery PET/CT 600, GE) with a spatial resolution of 5.1 mm FWHM at 60 min after FDG injection.

6.14.11 Image Interpretation

A swollen pancreatic tail and diffuse FDG uptake were seen (i). The salivary glands, especially the submandibular glands (g), systemic lymph nodes (h), para-aortic soft tissue (k), and prostate gland (l), all displayed abnormal FDG uptake. Bilateral swelling of the kidneys and abnormal accumulation in the cortical region were apparent (j). Physiological uptake in the ascending colon was seen.

6.14.12 Differential Diagnosis

IgG4-related disease, malignant lymphoma, pancreatic cancer with metastases, sarcoidosis, multicentric Castleman disease, vasculitis.

6.14.13 Diagnosis and Clinical Follow-Up

Kidney biopsy due to renal dysfunction revealed pathological findings of IgG4-related tubulointerstitial nephritis. Accordingly, he was diagnosed as having IgG4-related disease. Subsequent corticosteroid therapy improved his anemia and renal dysfunction.

6.14.14 Discussion

IgG4-related disease can manifest as autoimmune pancreatitis, sclerosing cholangitis, sialoadenitis, retroperitoneal fibrosis, interstitial nephritis, and other forms [133–135]. Excreted urinary FDG usually indicates high uptake in the kidney and urinary system. Moreover, high accumulation in the renal cortex is an abnormal finding on FDG-PET/CT that points to IgG4-related interstitial nephritis [136].

6.15 IgG4RD: Autoimmune Pancreatitis

Masatoyo Nakajo

Abstract The F-18-fluorodeoxyglucose (^{18}F-FDG) positron emission tomography (PET)/computed tomography (CT) findings before and after steroid treatment in a 69-year-old man with IgG4-related disease (IgG4-RD) were reported. Pretreatment ^{18}F-FDG PET/CT revealed abnormal ^{18}F-FDG uptake in the lacrimal glands, salivary glands, pleura, pancreas, and periaortic retroperitoneal region. Posttreatment ^{18}F-FDG PET/CT revealed reduced ^{18}F-FDG uptake in the lesions with abnormal ^{18}F-FDG uptake mentioned above. These ^{18}F-FDG PET/CT findings suggest the usefulness of ^{18}F-FDG PET/CT for assessing the extent of the disease and evaluating the treatment response of patients with IgG4-RD.

Keywords: IgG4-related disease, ^{18}F-FDG PET/CT, Diagnosis, Monitoring

6.15.1 Clinical Presentation

A 69-year-old man presented with a right upper eyelid mass. Excisional biopsy revealed the infiltration of IgG4-positive plasma cells with an IgG4/IgG ratio > 40%. Serum IgG4 was elevated at 1020 mg/dL (reference range: 4.8–105 mg/dL). Therefore, the patient was diagnosed with IgG4-RD, and a systematic work-up with ^{18}F-FDG PET/CT was performed.

6.15.2 Key Images (Fig. 6.23)

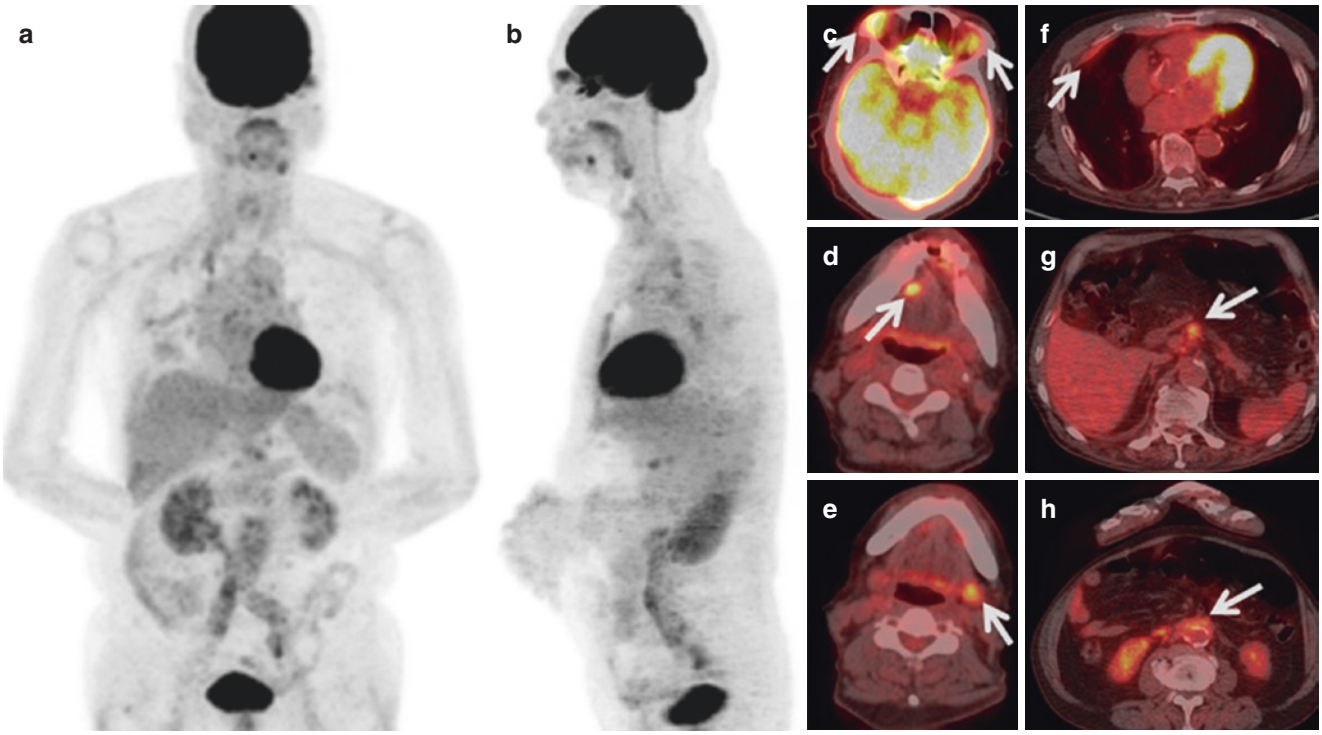

Fig. 6.23 18F-FDG PET/CT image

6.15.3 Technique

- Patient preparation: The patient was instructed to fast for ≥5 h before the administration of ^{18}F-FDG.
- Administrated dose of ^{18}F-FDG: 250 MBq.
- Imaging device: Whole-body PET/CT camera (Discovery 600 M PET/CT, GE Medical Systems) with a resolution of 5.1 mm of full-width at half-maximum.
- Image acquisition: Acquisition began 1 h after the intravenous injection of ^{18}F-FDG, and the images were obtained from brain to feet (acquisition time was 2.5 min per bed position with 14 bed positions) after CT using a 16-slice CT scanner (slice thickness, 3.75 mm; pitch, 1.75 mm; 120 keV; auto mA [35–100 mA depending on the patient body mass]).
- Reconstruction: Three-dimensional ordered-subset expectation maximization algorithm (image matrix size, 192 × 192; 16 subsets, 2 iterations: VUE Point Plus).

6.15.4 Image Interpretation

Pretreatment ^{18}F-FDG PET/CT maximum intensity projection (MIP) (Fig. 6.23a,b) and fused images showed increased abnormal ^{18}F-FDG uptake in the bilateral lacrimal glands (Fig. 6.23c, arrows), right sublingual gland (Fig. 6.23d, arrow), left submandibular gland (Fig. 6.23e, arrow), right pleura (Fig. 6.23f, arrow), proximal part of the pancreatic body (Fig. 6.23g, arrow), and periaortic retroperitoneal region (Fig. 6.23h, arrow).

6.15.5 Differential Diagnosis [137]

- Lymphoproliferative disorders
  - Malignant lymphoma
  - Multicentric Castleman disease
- Examples of other autoimmune diseases
  - Retroperitoneal fibrosis
  - Autoimmune pancreatitis

6.15.6 Diagnosis and Clinical Follow-Up (Fig. 6.24)

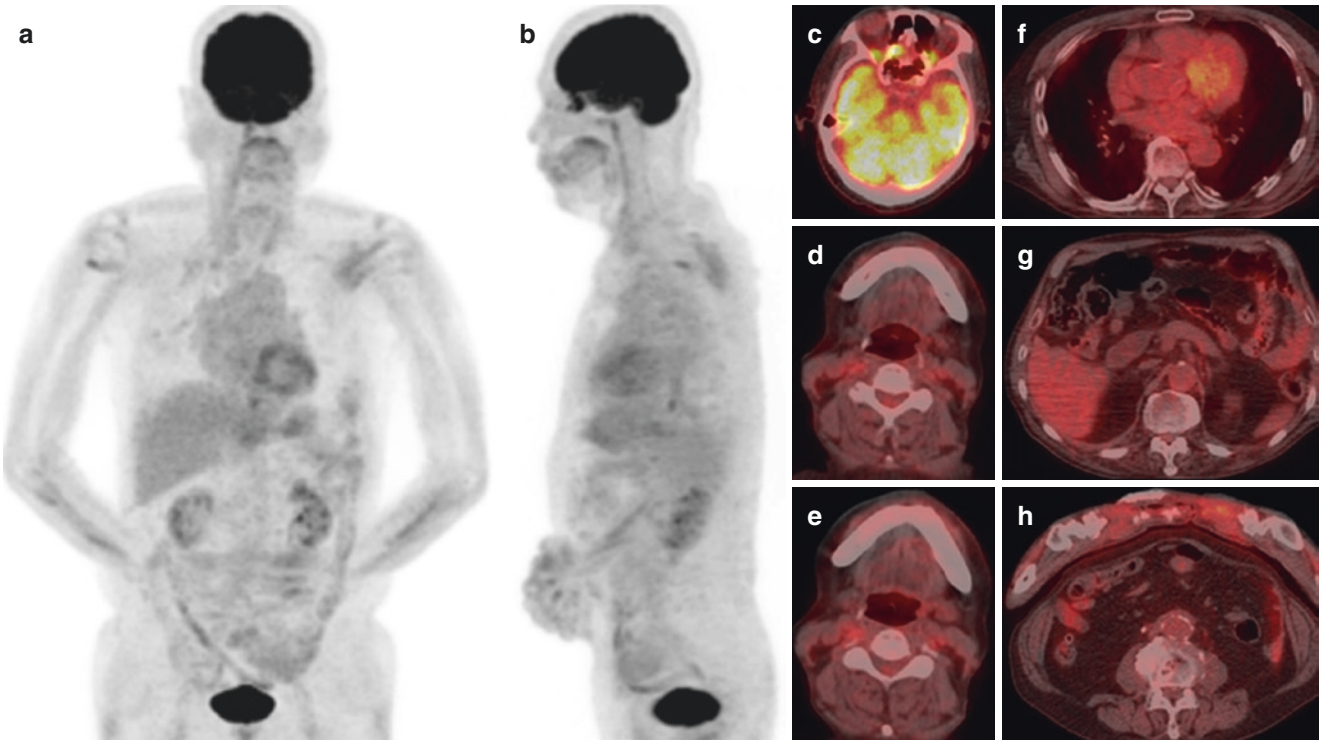

Fig. 6.24 Biopsy of the lacrimal glands confirmed the diagnosis of IgG4-RD, and oral glucocorticoid therapy was initiated. ^{18}F-FDG PET/CT MIP (**a**, **b**) with fused images after 6 months of treatment revealed that the abnormal uptake in the lacrimal glands (**c**), salivary glands (**d**, **e**), pleura (**f**), pancreas (**g**), and periaortic retroperitoneal region (**h**) almost completely disappeared, indicating a good treatment response. The serum IgG4 levels were normalized

6.15.7 Discussion

IgG4-RD is a systemic inflammatory disorder characterized by swollen lesions with lymphoplasmacytic infiltration of IgG4-positive plasma cells [138]. ^{18}F-FDG PET/CT is a whole-body examination that provides metabolic information about disease activity [139] The present case demonstrated the usefulness of ^{18}F-FDG PET/CT for assessing the extension disease and evaluating the treatment response of patients with IgG4-RD.

6.16 IgG4-Related Cardiovascular Disease (IgG4-CVD)

Noriko Oyama-Manabe

Abstract Immunoglobulin G4 (IgG4)–related disease can affect the cardiovascular system, including the coronary arteries and pericardium and especially the walls of large- and medium-sized vessels. The features of IgG4-related cardiovascular disease (IgG4-CVD) on CT include arterial wall thickening and homogeneous wall enhancement. Inflammatory abdominal aortic aneurysms are also attributed to a manifestation of IgG4-CVD. The entire aorta and major branches can be involved with more than twofold the FDG uptake of the venous background pool. Combining the metabolic information from FDG-PET/CT with the thickened vessel wall data from co-registered CECT could be a powerful method for evaluating inflammatory IgG4-CVD.

Keywords: IgG4-related disease, CT, FDG PET, Aortitis, Inflammatory aortic aneurysm

6.16.1 Clinical Presentation

83-year-old woman presenting with diabetes mellitus. Screening CT showed infra-renal abdominal aorta aneurysm (AAA).

6.16.2 Key Images

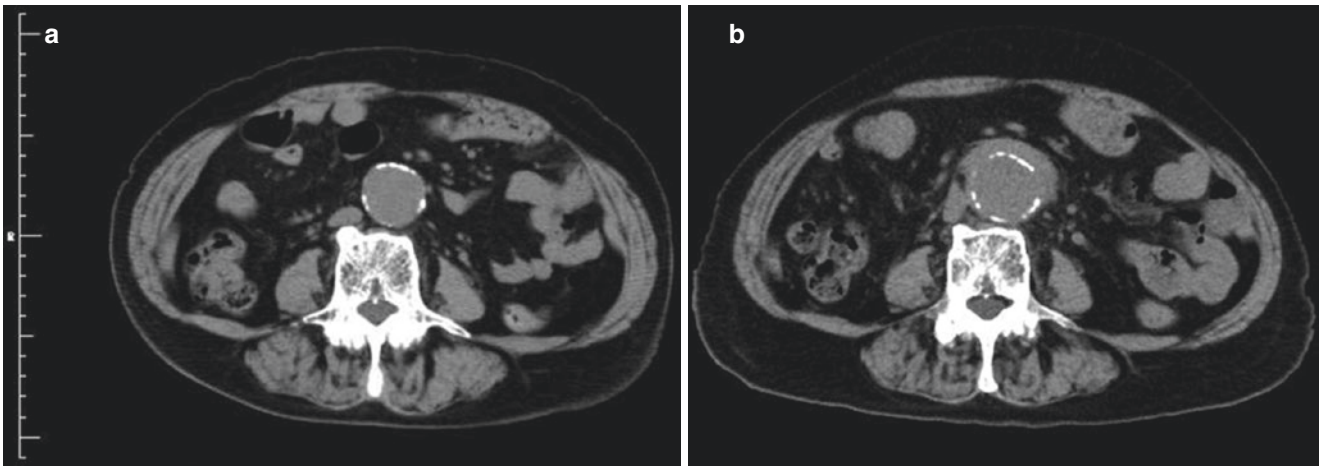

Fig. 6.25 Noncontrast CT

6.16.3 Technique

- Patient preparation: patient should not take anything by mouth for 6 h before administration of radiopharmaceutical.
- PET images were acquired 60 min after an intravenous injection of FDG (4–5 MBq/kg).
- Imaging device: whole body PET/CT camera (Biograph 64 with TrueV and high-definition PET, Siemens Japan, Tokyo).
- Emission scanning for 3 min per bed position was carried out following the CT image acquisition for attenuation corrections.

6.16.4 Image Interpretation

Initial noncontrast CT (Fig. 6.25a) demonstrates infra-renal AAA (31 × 30 mm). Four years later, follow-up CT (Fig. 6.25b) showed diffuse aortic wall thickness (maximal thickness 8 mm) and rapid progression in size (inner diameter 34 × 35 mm, outer diameter 46 × 42 mm).

6.16.5 Differential Diagnosis

- Atherosclerotic aortic aneurysm
- Infectious aortic aneurysm
- Inflammatory aortic aneusysm
- Impending rupture of the aortic aneurysm

6.16.6 Diagnosis and Clinical Follow-Ups (Fig. 6.26)

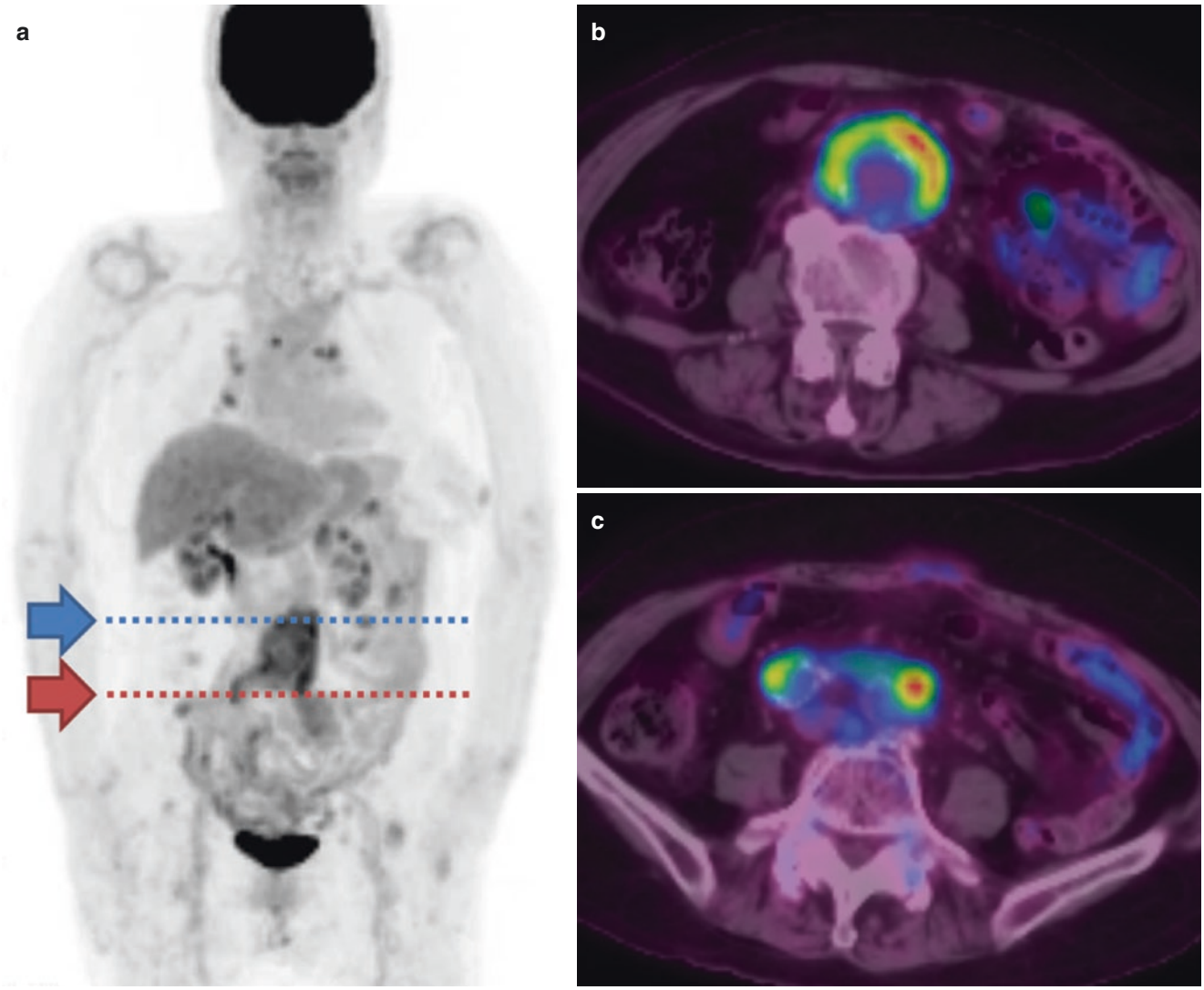

Fig. 6.26 Maximum intensity projection image (**a**) and axial fused images at AAA (**b**, blue arrow level) and common iliac arteries (**c**, red arrow level) are displayed. Strong focal uptakes on AAA (SUV_{max} = 4.9) and common iliac arteries (SUV_s = 5.9) which represented the active inflammation. Aortic replacement was held. There were lymphoplasmacytic infiltration and extensive dense infiltration of IgG4-positive plasma cells within the aortic wall, mainly in the adventitia, which was concordant with IgG4-related inflammatory aneurysm

6.16.7 Discussion

The metabolic information from FDG-PET/CT could be a powerful method for evaluating inflammatory IgG4-aortitis [140, 141]. The infra-renal abdominal aorta and iliac arteries were the most commonly involved sites with more than twice the FDG uptake as compared to the venous blood pool, which could form aneurysmal change [141].

References

1. Boers M, Verhoeven AC, Markusse HM, van de Laar MA, Westhovens R, van Denderen JC, et al. Randomised comparison of combined step-down prednisolone, methotrexate and sulphasalazine with sulphasalazine alone in early rheumatoid arthritis. Lancet. 1997;350:309–18.
2. Landewé RB, Boers M, Verhoeven AC, Westhovens R, van de Laar MA, Markusse HM, , et al. COBRA combination therapy in patients with early rheumatoid arthritis: long-term structural benefits of a brief intervention**.** Arthritis Rheum 2002;46: 347–356.
3. McQueen FM, Stewart N, Crabbe J, Robinson E, Yeoman S, Tan PL, et al. Magnetic resonance imaging of the wrist in early rheumatoid arthritis reveals a high prevalence of erosions at four months after symptom-onset. Ann Rheum Dis. 1998;57: 350–6.
4. Ostergaard M, Hansen M, Stoltenberg M, Gideon P, Klarlund M, Jensen KE, et al. Magnetic resonance imaging-determined synovial membrane volume as a marker of disease activity and a predictor of progressive joint destruction in the wrists of patients with rheumatoid arthritis. Arthritis Rheum. 1999;42:918–29.
5. Kane D, Balint PV, Sturrock RD. Ultrasonography is superior to clinical examination in the detection and localization of knee joint effusion in rheumatoid arthritis. J Rheumatol. 2003;30:966–71.
6. Koenigkam-Santos M, Sharma P, Kalb B, Oshinski JN, Weyand CM, Goronzy JJ, et al. Magnetic resonance angiography in extracranial giant cell arteritis. J Clin Rheumatol. 2011;17:306–10.
7. Kubota R, Yamada S, Kubota K, Ishiwata K, Tamahashi N, Ido T. Intratumoral distribution of flurine-18-fluorodeoxyglucose in vivo: high accumulation in macrophages and granulation tissues studied by microautoradiography. J Nucl Med. 1992;33:1972–80.
8. Yamada S, Kubota K, Kubota R, Ido T, Tamahashi N. High accumulation of fluorine-18-fluorodeoxyglucose in turpentine-induced inflammatory tissue. J Nucl Med. 1995;36:1301–6.
9. Matsui T, Nakata N, Nagai S, Nakatani A, Takahashi M, Momose T, et al. Inflammatory cytokines and hypoxia contribute to 18F-FDG uptake by cells involved in pannus formation in rheumatoid arthritis. J Nucl Med. 2009;50:920–6.
10. Palmer WE, Rosenthal DI, Schoenberg OI, Fischman AJ, Simon LS, Rubin RH, et al. Quantification of inflammation in the wrist with gadolinium-enhanced MR imaging and PET with 2-[F-18]-fluoro-2-deoxy-D-glucose. Radiology. 1995;196:647–55.
11. Beckers C, Ribbens C, André B, Marcelis S, Kaye O, Mathy L, et al. Assessment of disease activity in rheumatoid arthritis with (18)F-FDG PET. J Nucl Med. 2004;45:956–64.
12. Kubota K, Ito K, Morooka M, Mitsumoto T, Kurihara K, Yamashita H, et al. Whole-body FDG-PET/CT on rheumatoid arthritis of large joints. Ann Nucl Med. 2009;23:783–91.
13. Goerres GW, Forster A, Uebelhart D, Seifert B, Treyer V, Michel B, , et al. F-18 FDG whole-body PET for the assessment of disease activity in patients with rheumatoid arthritis**.** Clin Nucl Med 2006;31:386–390.
14. Elzinga EH, van der Laken CJ, Comans EF, Lammertsma AA, Dijkmans BA, Voskuyl AE. 2-Deoxy-2-[F-18]fluoro-D-glucose joint uptake on positron emission tomography images: rheumatoid arthritis versus osteoarthritis. Mol Imaging Biol. 2007;9:357–60.
15. Ostendorf B, Mattes-György K, Reichelt DC, Blondin D, Wirrwar A, Lanzman R, et al. Early detection of bony alterations in rheumatoid and erosive arthritis of finger joints with high-resolution single photon emission computed tomography, and differentiation between them. Skelet Radiol. 2010;39:55–61.
16. Okabe T, Shibata H, Shizukuishi K, Yoneyama T, Inoue T, Tateishi U. F-18 FDG uptake patterns and disease activity of collagen vascular diseases-associated arthritis. Clin Nucl Med. 2011;36:350–4.
17. Beckers C, Jeukens X, Ribbens C, André B, Marcelis S, Leclercq P, et al. (18)F-FDG PET imaging of rheumatoid knee synovitis correlates with dynamic magnetic resonance and sonographic assessments as well as with the serum level of metalloproteinase-3. Eur J Nucl Med Mol Imaging. 2006;33:275–80.
18. Sato M, Inubushi M, Shiga T, Hirata K, Okamoto S, Kamibayashi T, et al. Therapeutic effects of acupuncture in patients with rheumatoid arthritis: a prospective study using (18)F-FDG-PET. Ann Nucl Med. 2009;23:311–6.
19. Brown AK, Conaghan PG, Karim Z, Quinn MA, Ikeda K, Peterfy CG, et al. An explanation for the apparent dissociation between clinical remission and continued structural deterioration in rheumatoid arthritis. Arthritis Rheum. 2008;58:2958–67.
20. Elzinga EH, van der Laken CJ, Comans EF, Boellaard R, Hoekstra OS, Dijkmans BA, et al. 18F-FDG PET as a tool to predict the clinical outcome of infliximab treatment of rheumatoid arthritis: an explorative study. J Nucl Med. 2011;52:77–80.
21. Polisson RP, Schoenberg OI, Fischman A, Rubin R, Simon LS, Rosenthal D, et al. Use of magnetic resonance imaging and positron emission tomography in the assessment of synovial volume and glucose metabolism in patients with rheumatoid arthritis. Arthritis Rheum. 1995;38:819–25.
22. Adams MC, Turkington TG, Wilson JM, Wong TZ. A systematic review of the factors affecting accuracy of SUV measurements. AJR Am J Roentgenol. 2010;195:310–20.
23. Szkudlarek M, Court-Payen M, Jacobsen S, Klarlund M, Thomsen HS, Østergaard M. Interobserver agreement in ultrasonography of the finger and toe joints in rheumatoid arthritis. Arthritis Rheum. 2003;48:955–62.
24. Kubota K, Ito K, Morooka M, Minamimoto R, Miyata Y, Yamashita H, et al. FDG PET for rheumatoid arthritis: basic considerations and whole-body PET/CT. Ann N Y Acad Sci. 2011;1228:29–38.
25. Miese F, Scherer A, Ostendorf B, Heinzel A, Lanzman RS, Kröpil P, et al. Hybrid 18F-FDG PET-MRI of the hand in rheumatoid arthritis: initial results. Clin Rheumatol. 2011;30:1247–50.
26. Suto T, Okamura K, Yonemoto Y, Okura C, Tsushima Y, Takagishi K. Prediction of large joint destruction in patients with rheumatoid arthritis using 18F-FDG PET/CT and disease activity score. Medicine (Baltimore). 2016;95:e2841.
27. Suto T, Yonemoto Y, Okamura K, Okura C, Kaneko T, Kobayashi T, et al. Predictive factors associated with the progression of large-joint destruction in patients with rheumatoid arthritis after biologic therapy: a post-hoc analysis using FDG-PET/CT and the ARASHI (assessment of rheumatoid arthritis by scoring of large-joint destruction and healing in radiographic imaging) scoring method. Mod Rheumatol. 2017;27:820–7.
28. Chuang TY, Hunder GG, Ilstrup DM, Kurland LT. Polymyalgia rheumatica: a 10-year epidemiologic and clinical study. Ann Intern Med. 1982;97:672–80.
29. Healey LA. Long-term follow-up of polymyalgia rheumatica: evidence for synovitis. Semin Arthritis Rheum. 1984;13:322–8.
30. Salvarani C, Cantini F, Olivieri I, Hunder GS. Polymyalgia rheumatica: a disorder of extraarticular synovial structures? J Rheumatol. 1999;26:517.

31. Salvarani C, Cantini F, Olivieri I, Barozzi L, Macchioni L, Niccoli L, et al. Proximal bursitis in active polymyalgia rheumatica. Ann Intern Med. 1997;127:27–31.
32. Cantini F, Salvarani C, Olivieri I, Niccoli L, Padula A, Macchioni L, et al. Shoulder ultrasonography in the diagnosis of polymyalgia rheumatica: a case–control study. J Rheumatol. 2001;28:1049–55.
33. Moosig F, Czech N, Mehl C, Henze E, Zeuner RA, Kneba M, et al. Correlation between 18-fluorodeoxyglucose accumulation in large vessels and serological markers of inflammation in polymyalgia rheumatica: a quantitative PET study. Ann Rheum Dis. 2004;63:870–3.
34. Blockmans D, De Ceuninck L, Vanderschueren S, Knockaert D, Mortelmans L, Bobbaers H. Repetitive 18-fluorodeoxyglucose positron emission tomography in isolated polymyalgia rheumatica: a prospective study in 35 patients. Rheumatology (Oxford). 2007;46:672–7.
35. Yamashita H, Kubota K, Takahashi Y, Minamimoto R, Morooka M, Ito K, et al. Whole-body fluorodeoxyglucose positron emission tomography/computed tomography in patients with active polymyalgia rheumatica: evidence for distinctive bursitis and large-vessel vasculitis. Mod Rheumatol. 2012;22:705–11.
36. Takahashi H, Yamashita H, Kubota K, Miyata Y, Okasaki M, Morooka M, et al. Differences in fluorodeoxyglucose positron emission tomography/computed tomography findings between elderly onset rheumatoid arthritis and polymyalgia rheumatica. Mod Rheumatol. 2015;25:546–51.
37. Cimmino MA, Camellino D, Paparo F, Morbelli S, Massollo M, Cutolo M, et al. High frequency of capsular knee involvement in polymyalgia rheumatica/giant cell arteritis patients studied by positron emission tomography. Rheumatology (Oxford). 2013;52:1865–72.
38. Wakura D, Kotani T, Takeuchi T, Komori T, Yoshida S, Makino S, et al. Differentiation between polymyalgia rheumatica (PMR) and elderly-onset rheumatoid arthritis using 18F-Fluorodeoxyglucose positron emission tomography/computed tomography: is enthesitis a new pathological lesion in PMR? PLoS One. 2016;11:e0158509.
39. Owen CE, Poon AMT, Lee ST, Yap LP, Zwar RB, McMenamin CM, et al. Fusion of positron emission tomography/computed tomography with magnetic resonance imaging reveals hamstring peritendonitis in polymyalgia rheumatica. Rheumatology (Oxford). 2018;57:345–53.
40. Rehak Z, Vasina J, Nemec P, Fojtik Z, Koukalova R, Bortlicek Z, et al. Various forms of (18)F-FDG PET and PET/CT findings in patients with polymyalgia rheumatica. Biomed Pap Med Fac Univ Palacky Olomouc Czech Repub. 2015;159:629–36.
41. Rehak Z, Sprlakova-Pukova A, Bortlicek Z, Fojtik Z, Kazda T, Joukal M, et al. PET/CT imaging in polymyalgia rheumatica: praepubic 18F-FDG uptake correlates with pectineus and adductor longus muscles enthesitis and with tenosynovitis. Radiol Oncol. 2017;51:8–14.
42. Camellino D, Paparo F, Morbelli S, Cutolo M, Sambuceti G, Cimmino MA. Interspinous bursitis is common in polymyalgia rheumatica, but is not associated with spinal pain. Arthritis Res Ther. 2014;16:492.
43. Palard-Novello X, Querellou S, Gouillou M, Saraux A, Marhadour T, Garrigues F, et al. Value of (18)F-FDG PET/CT for therapeutic assessment of patients with polymyalgia rheumatica receiving tocilizumab as first-line treatment. Eur J Nucl Med Mol Imaging. 2016;43:773–9.
44. Nash P, Mease PJ, Braun J, van der Heijde D. Seronegative spondyloarthropathies: to lump or split? Ann Rheum Dis. 2005;64(Suppl. II):9–13.
45. Godfrin B, Zabraniecki L, Lamboley V, Bertrand-Latour F, Sans N, Fournié B. Spondyloarthropathy with entheseal pain. A prospective study in 33 patients. Joint Bone Spine. 2004;71:557–62.
46. Taniguchi Y, Arii K, Kumon Y, Fukumoto M, Ohnishi T, Horino T, et al. Positron emission tomography/computed tomography: a clinical tool for evaluation of enthesitis in patients with spondyloarthritides. Rheumatology (Oxford). 2010;49:348–54.
47. Strobel K, Fischer DR, Tamborrini G, Kyburz D, Stumpe KD, Hesselmann RG, et al. 18F-fluoride PET/CT for detection of sacroiliitis in ankylosing spondylitis. Eur J Nucl Med Mol Imaging. 2010;37:1760–5.
48. Yamashita H, Kubota K, Takahashi Y, Minamimoto R, Morooka M, Kaneko H, et al. Similarities and differences in fluorodeoxyglucose positron emission tomography/computed tomography findings in spondyloarthropathy, polymyalgia rheumatica and rheumatoid arthritis. Joint Bone Spine. 2013;80:171–7.
49. Vijayant V, Sarma M, Aurangabadkar H, Bichile L, Basu S. Potential of (18)F-FDG-PET as a valuable adjunct to clinical and response assessment in rheumatoid arthritis and seronegative spondyloarthropathies. World J Radiol. 2012;4:462–8.
50. Bruijnen ST, van der Weijden MA, Klein JP, Hoekstra OS, Boellaard R, van Denderen JC, et al. Bone formation rather than inflammation reflects ankylosing spondylitis activity on PET-CT: a pilot study. Arthritis Res Ther. 2012;14:R71.
51. Lee SG, Kim IJ, Kim KY, Kim HY, Park KJ, Kim SJ, et al. Assessment of bone synthetic activity in inflammatory lesions and syndesmophytes in patients with ankylosing spondylitis: the potential role of 18F-fluoride positron emission tomography-magnetic resonance imaging. Clin Exp Rheumatol. 2015;33:90–7.
52. Buchbender C, Ostendorf B, Ruhlmann V, Heusch P, Miese F, Beiderwellen K, et al. Hybrid 18F-labeled fluoride positron emission tomography/magnetic resonance (MR) imaging of the sacroiliac joints and the spine in patients with axial Spondyloarthritis: a pilot study exploring the link of MR bone pathologies and increased Osteoblastic activity. J Rheumatol. 2015;42:1631–7.
53. Takata T, Takahashi A, Taniguchi Y, Terada Y, Sano S. Detection of asymptomatic enthesitis in psoriasis patients: an onset of psoriatic arthritis? J Dermatol. 2016;43:650–4.
54. Chaudhari AJ, Ferrero A, Godinez F, Yang K, Shelton DK, Hunter JC, et al. High-resolution (18)F-FDG PET/CT for assessing disease activity in rheumatoid and psoriatic arthritis: findings of a prospective pilot study. Br J Radiol. 2016;89:20160138.
55. Idolazzi L, Salgarello M, Gatti D, Viapiana O, Vantaggiato E, Fassio A, et al. 18F-fluoride PET/CT for detection of axial involvement in ankylosing spondylitis: correlation with disease activity. Ann Nucl Med. 2016;30:430–4.
56. Park EK, Pak K, Park JH, Kim K, Kim SJ, Kim IJ, et al. Baseline increased 18F-fluoride uptake lesions at vertebral corners on positron emission tomography predict new syndesmophyte development in ankylosing spondylitis: a 2-year longitudinal study. Rheumatol Int. 2017;37:765–73.
57. Sawicki LM, Lütje S, Baraliakos X, Braun J, Kirchner J, Boos J, et al. Dual-phase hybrid 18 F-fluoride positron emission tomography/MRI in ankylosing spondylitis: investigating the link between MRI bone changes, regional hyperaemia and increased osteoblastic activity. J Med Imaging Radiat Oncol. 2018;62:313–9.
58. Yamashita H, Takahashi Y, Kubota K, et al. Utility of fluorodeoxyglucose positron emission tomography/computed tomography for early diagnosis and evaluation of disease activity of relapsing polychondritis: a case series and literature review. Rheumatology (Oxford). 2014;53:1482–90.
59. Lei W, Zeng H, Zeng DX, Zhang B, Zhu YH, Jiang JH, et al. (18) F-FDG PET-CT: a powerful tool for the diagnosis and treatment of relapsing polychondritis. Br J Radiol. 2016;89(1057):20150695. https://doi.org/10.1259/bjr.20150695. Epub 2015 Nov 3.5
60. Yamashita H, Kubota K, Takahashi Y, et al. Clinical value of 18F-fluoro-dexoxyglucose positron emission tomography/computed tomography in patients with adult-onset Still's disease: a

seven-case series and review of the literature. Mod Rheumatol. 2013;24:645–50.
61. Dong MJ, Wang CQ, Zhao K, Wang GL, Sun ML, Liu ZF, et al. 18F-FDG PET/CT in patients with adult-onset Still's disease. Clin Rheumatol. 2015;34:2047–56.
62. Treglia G, Mattoli MV, Leccisotti L, Ferraccioli G, Giordano A. Usefulness of whole-body fluorine-18-fluorodeoxyglucose positron emission tomography in patients with large-vessel vasculitis: a systematic review. Clin Rheumatol. 2011;30:1265–75.
63. Muto G, Yamashita H, Takahashi Y, Miyata Y, Morooka M, Minamimoto R, Kubota K, Kaneko H, Kano T, Mimori A. Large vessel vasculitis in elderly patients: early diagnosis and steroid-response evaluation with FDG-PET/CT and contrast-enhanced CT. Rheumatol Int. 2014;34:1545–54.
64. Umehara H, Okazaki K, Masaki Y, Kawano M, Yamamoto M, Saeki T, et al. A novel clinical entity, IgG4-related disease (IgG4RD): general concept and details. Mod Rheumatol. 2012;22:1–14.
65. Shigekawa M, Yamao K, Sawaki A, Hara K, Takagi T, Bhatia V, et al. Is 18F-fluorodeoxyglucose positron emission tomography meaningful for estimating the efficacy of corticosteroid therapy in patients with autoimmune pancreatitis? J Hepatobiliary Pancreat Sci. 2010;17:269–74.
66. Ozaki Y, Oguchi K, Hamano H, Arakura N, Muraki T, Kiyosawa K, et al. Differentiation of autoimmune pancreatitis from suspected pancreatic cancer by fluorine-18 fluorodeoxyglucose positron emission tomography. J Gastroenterol. 2008;43:144–51.
67. Ebbo M, Grados A, Guedj E, Gobert D, Colavolpe C, Zaidan M, et al. 18F-FDG PET/CT for staging and evaluation of treatment response in IgG4-related disease: a retrospective multicenter study. Arthritis Care Res (Hoboken). 2014;66:86–96.
68. Takahashi H, Yamashita H, Morooka M, Kubota K, Takahashi Y, Kaneko H, Kano T, Mimori A. The utility of FDG-PET/CT and other imaging techniques in the evaluation of IgG4-related disease. Joint Bone Spine. 2014. pii: S1297-319X(14)00031-1. [Epub ahead of print]; https://doi.org/10.1016/j.jbspin.2014.01.010.
69. Tokue A, Higuchi T, Arisaka Y, Nakajima T, Tokue H, Tsushima Y. Role of F-18 FDG PET/CT in assessing IgG4-related disease with inflammation of head and neck glands. Ann Nucl Med. 2015;29:499–505.
70. Lauwyck J, Piette Y, Van Walleghem L, De Geeter F. IgG4-related disease: the utility of (18)F-FDG PET/CT in diagnosis and treatment. Hell J Nucl Med. 2015;18(Suppl 1):155–9.
71. Zhao Z, Wang Y, Guan Z, Jin J, Huang F, Zhu J. Utility of FDG-PET/CT in the diagnosis of IgG4-related diseases. Clin Exp Rheumatol. 2016;34:119–25.
72. Lee J, Hyun SH, Kim S, Kim DK, Lee JK, Moon SH, et al. Utility of FDG PET/CT for differential diagnosis of patients clinically suspected of IgG4-related disease. Clin Nucl Med. 2016;41:e237–43.
73. Martinez-Pimienta G, Noriega-Álvarez E, Simó-Perdigó M. Study of systemic disease IgG4. Usefulness of 2-[18F]-fluoro-2-deoxy-D-glucose -positron emission tomography/computed tomography for staging, selection of biopsy site, evaluation of treatment response and follow-up. Eur J Rheumatol. 2017;4:222–5.
74. Berti A, Della-Torre E, Gallivanone F, Canevari C, Milani R, Lanzillotta M, et al. Quantitative measurement of 18F-FDG PET/CT uptake reflects the expansion of circulating plasmablasts in IgG4-related disease. Rheumatology (Oxford). 2017;56:2084–92.
75. Takano K, Yajima R, Kamekura R, Yamamoto M, Takahashi H, Yama N, et al. Clinical utility of 18 F-fluorodeoxyglucose/positron emission tomography in diagnosis of immunoglobulin G4-related sclerosing sialadenitis. Laryngoscope. 2018;128:1120–5.
76. Owada T, Maezawa R, Kurasawa K, Okada H, Arai S, Fukuda T. Detection of inflammatory lesions by f-18 fluorodeoxyglucose positron emission tomography in patients with polymyositis and dermatomyositis. J Rheumatol. 2012;39:1659–65.
77. Tanaka S, Ikeda K, Uchiyama K, et al. [18F]FDG uptake in proximal muscles assessed by PET/CT reflects both global and local muscular inflammation and provides useful information in the management of patients with polymyositis/dermatomyositis. Rheumatology (Oxford). 2013;52:1271–8.
78. Matuszak J, Blondet C, Hubelé F, Gottenberg JE, Sibilia J, Bund C, et al. Muscle fluorodeoxyglucose uptake assessed by positron emission tomography-computed tomography as a biomarker of inflammatory myopathies disease activity. Reumatology (Oxford). 2019. pii: kez040. [Epub ahead of print]; https://doi.org/10.1093/rheumatology/kez040.
79. Motegi SI, Fujiwara C, Sekiguchi A, Hara K, Yamaguchi K, Maeno T. Clinical value of 18 F-fluorodeoxyglucose positron emission tomography/computed tomography for interstitial lung disease and myositis in patients with dermatomyositis. J Dermatol. 2019;46:213–8.
80. Sun L, Dong Y, Zhang N, Lv X, Chen Q, Wei W. [18F] Fluorodeoxyglucose positron emission tomography/computed tomography for diagnosing polymyositis/dermatomyositis. Exp Ther Med. 2018;15:5023–8.
81. Tateyama M, Fujihara K, Misu T, Arai A, Kaneta T, Aoki M. Clinical values of FDG PET in polymyositis and dermatomyositis syndromes: imaging of skeletal muscle inflammation. BMJ Open. 2015;5:e006763.
82. Soussan M, Abisror N, Abad S, Nunes H, Terrier B, Pop G, et al. FDG-PET/CT in patients with ANCA-associated vasculitis: case-series and literature review. Autoimmun Rev. 2014;13:125–31.
83. Nelson DR, Johnson GB, Cartin-Ceba R, Specks U. Characterization of F-18 fluorodeoxyglucose PET/CT in granulomatosis with polyangiitis. Sarcoidosis Vasc Diffuse Lung Dis. 2016;32:342–52.
84. Kemna MJ, Bucerius J, Drent M, Vöö S, Veenman M, van Paassen P, et al. Aortic ^{18}F-FDG uptake in patients suffering from granulomatosis with polyangiitis. Eur J Nucl Med Mol Imaging. 2015;42:1423–9.
85. Lei J, Yan X, Taoying G, et al. Imaging characteristics of adult onset Still's disease demonstrated with ^{18}F-FDG PET/CT. Mol Med Rep. 2017;16(3):3680–6.
86. Yaguchi D, Inoue N, Koike W, et al. FDG-PET/CT findings in adult-onset Still's disease. QJM. 2019;112:705–6. pii: hcz057
87. Owada T, Maezawa R, Kurasawa K, et al. Detection of inflammatory lesions by F-18 Fluorodeoxyglucose positron emission tomography in patients with polymyositis and dermatomyositis. J Rheumatol. 2012;39(8):1659–65.
88. Sun L, Dong Y, Zhang N, et al. [^{18}F]Fluorodeoxyglucose positron emission tomography/computed tomography for diagnosing polymyositis/dermatomyositis. Exp Ther Med. 2018;15(6):5023–8.
89. Maliha PG, Hudson M, Abikhzer G, et al. ^{18}F-FDG PET/CT versus conventional investigations for cancer screening in autoimmune inflammatory myopathy in the era of novel myopathy classifications. Nucl Med Commun. 2019;40(4):377–82.
90. Tateyama M, Fujihara K, Misu T, et al. Clinical values of FDG PET in polymyositis and dermatomyositis syndromes: imaging of skeletal muscle inflammation. BMJ Open. 2015;5(1):e006763.
91. Bai X, Tie N, Wang X, et al. Intense muscle activity due to polymyositis incidentally detected in a patient evaluated for possible malignancy by FDG PET/CT imaging. Clin Nucl Med. 2017;42(8):647–8.
92. Khan S, Christopher-Stine L. Polymyositis, dermatomyositis, and autoimmune necrotizing myopathy: clinical features. Rheum Dis Clin N Am. 2011;37(2):143–58.
93. Horino T, Matsumoto T, Ichii O, et al. Long-term imaging findings on serial FDG PET/CT scans in a patient with polymyositis. J Clin Rheumatol. 2019;. [Epub ahead of print]

94. Tanaka S, Ikeda K, Uchiyama K, et al. [18 F] FDG uptake in proximal muscles assessed by PET/CT reflects both global and local muscular inftammation and provides useful information in the management of patients with polymyositis/dermatomyositis. Rheumatology. 2013;52(7):1271–8.
95. Matuszak J, Blondet C, Hubelé F, et al. Muscle fluorodeoxyglucose uptake assessed by positron emission tomography-computed tomography as a biomarker of inflammatory myopathies disease activity. Rheumatology (Oxford). 2019 Mar 8. pii: kez040.
96. Mahmood S, Rodríguez Martínez de Llano S. ^{18}F-FDG PET detection of unknown primary malignancy in dermatomyositis. Clin Nucl Med. 2012;37(8):e204–5.
97. Pei L, Guan ZW, Ji XJ, et al. The application of ^{18}F fluorodeoxyglucose-positron emission tomography/computed tomography in the diagnosis and treatment of dermatomyositis. Zhonghua Nei Ke Za Zhi. 2016;55(7):525–30.
98. Motegi SI, Fujiwara C, Sekiguchi A, et al. Clinical value of ^{18}F-fluorodeoxyglucose positron emission tomography/computed tomography for interstitial lung disease and myositis in patients with dermatomyositis. J Dermatol. 2019;46(3):213–8.
99. Tanaka S, Ikeda K, Uchiyama K, et al. ^{18}FDG uptake in proximal muscles assessed by PET/CT reflects both global and local muscular inflammation and provides useful information in the management of patients with polymyositis/dermatomyositis. Rheumatology. 2013;52(7):1271–8.
100. Kundrick A, Kirby J, Ba D, et al. Positron emission tomography costs less to patients than conventional screening for malignancy in dermatomyositis. Semin Arthritis Rheum. 2018;49:140–4. S0049-0172(18)30107-0
101. Lazarou IN, et al. Classification, diagnosis, and management of idiopathic inflammatory myopathies. J Rheumatol. 2013;40:550–64.
102. Hill C, et al. Frequency of specific cancer types in dermatomyositis and polymyositis: a population based study. Lancet. 2001;357:96–100.
103. Tateyama M, et al. Clinical values of FDG PET in polymyositis and dermatomyositis syndromes: imaging of skeletal muscle inflammation. BMJ Open. 2015;12:5.
104. Li Y, et al. Multiple values of (18)F-FDG PET/CT in idiopathic inflammatory myopathy. Clin Rheumatol. 2017;36:2297–305.
105. Motegi S, et al. Clinical value of (18)F-fluorodeoxyglucose positron emission tomography/computed tomography for interstitial lung disease and myositis in patients with dermatomyositis. J Dermatol. 2019;46:213–8.
106. Kubota K, et al. Whole-body FDG-PET/CT on rheumatoid arthritis of large joints. Ann Nucl Med. 2009;23:783–91.
107. Kubota K, et al. FDG PET for rheumatoid arthritis: basic considerations and whole-body PET/CT. Ann N Y Acad Sci. 2011;1228:29–38.
108. Goerres GW, et al. F-18 FDG whole-body PET for the assessment of disease activity in patients with rheumatoid arthritis. Clin Nucl Med. 2006;31:386–90.
109. Yamashita H, et al. Clinical value of whole-body PET/CT in patients with active rheumatic diseases. Arthritis Res Ther. 2014;16:423.
110. Beckers C, Ribbens C, André B, et al. Assessment of disease activity in rheumatoid arthritis with ^{18}F-FDG PET. J Nucl Med. 2004;45(6):956–64.
111. Goerres GW, Forster A, Uebelhart D, et al. F-18 FDG whole-body PET for the assessment of disease activity in patients with rheumatoid arthritis. Clin Nucl Med. 2006;31(7):386–90.
112. Matsui T, Nakata N, Nagai S, et al. Inflammatory cytokines and hypoxia contribute to ^{18}F-FDG uptake by cells involved in pannus formation in rheumatoid arthritis. J Nucl Med. 2009;50(6):920–6.
113. Lee SJ, Jeong JH, Lee CH, et al. Development and validation of an ^{18}F-FDG PET/CT-based tool for the evaluation of joint counts and disease activity in patients with rheumatoid arthritis. Arthritis Rheumatol. 2019;71:1232–40. [Epub ahead of print]
114. Yamashita H, et al. Whole-body fluorodeoxyglucose positron emission tomography/computed tomography in patients with active polymyalgia rheumatica: evidence for distinctive bursitis and large-vessel vasculitis. Mod Rheumatol. 2012;22:705–11.
115. Takahashi H, et al. Differences in fluorodeoxyglucose positron emission tomography/computed tomography findings between elderly onset rheumatoid arthritis and polymyalgia rheumatica. Mod Rheumatol. 2015;25(54):6–51.
116. Yamashita H, et al. Utility of fluorodeoxyglucose positron emission tomography/computed tomography for early diagnosis and evaluation of disease activity of relapsing polychondritis: a case series and literature review. Rheumatology (Oxford). 2014;53:1482.
117. Deng H, et al. Relapsing polychondritis on PET/CT. Clin Nucl Med. 2012;37:712.
118. De Geeter F, Gykiere P. 18F-FDG PET/CT imaging in granulomatosis with polyangiitis. Hell J Nucl Med. 2016;19(1):5–6.
119. De Geeter F, Gykiere P. 18F-FDG PET imaging of granulomatosis with polyangiitis –Wegener's syndrome. Hell J Nucl Med. 2016;19(1):53–6.
120. Bonnet P, Abisror N, Fain O, et al. 18FDG PET for detecting renal granulomatous localization: illustration of granulomatosis with polyangiitis and sarcoidosis. J Clin Rheumatol. 2019;. [Epub ahead of print]
121. Fu Z, Liu M, Li Z, et al. Occult renal granulomatous inflammatory lesions in granulomatosis with polyangiitis detected by 18F-FDG PET/CT. Clin Nucl Med. 2017;42(9):707–8.
122. Ito K, et al. Evaluation of Wegener's granulomatosis using 18F-fluorodeoxyglucose positron emission tomography/computed tomography. Ann Nucl Med. 2013;27(3):209–16.
123. Ozmen O, et al. Integration of 2-deoxy-2-[18F] fluoro-D-glucose PET/CT into clinical management of patients with Wegener's granulomatosis. Ann Nucl Med. 2013;27(10):907–15.
124. Kemna MJ, et al. Aortic ^{18}F-FDG uptake in patients suffering from granulomatosis with polyangiitis. Eur J Nucl Med Mol Imaging. 2015;42(9):1423–9.
125. Nelson DR, et al. Characterization of F-18 fluorodeoxyglucose PET/CT in granulomatosis with polyangiitis. Sarcoidosis Vasc Diffuse Lung Dis. 2016;32(4):342–52.
126. Perel-Winkler A, Bokhari S, Perez-Recio T, et al. Myocarditis in systemic lupus erythematosus diagnosed by ^{18}F-fluorodeoxyglucose positron emission tomography. Lupus Sci Med. 2018;5(1):e000265.
127. Makis W, Ciarallo A, Gonzalez-Verdecia M, et al. Systemic lupus Erythematosus associated pitfalls on ^{18}F-FDG PET/CT: reactive follicular hyperplasia, Kikuchi-Fujimoto disease, inflammation and lymphoid hyperplasia of the spleen mimicking lymphoma. Nucl Med Mol Imaging. 2018;52(1):74–9.
128. Girard A, Ohnona J, Bernaudin JF, et al. Generalized lymph node FDG uptake as the first manifestation of systemic lupus erythematosus. Clin Nucl Med. 2017;42(10):787–9.
129. Ozaki Y, et al. Differentiation of autoimmune pancreatitis from suspected pancreatic cancer by floutrine-18 fluorodeoxylucose positron emission tomogramphy. J Gastroenterol. 2008;43(2):144–51.
130. Sato M, et al. Extrapancreatic F-18 FDG accumulateon in autoimmune pancreastitis. Ann Nucl Med. 2008;22(3):215–9.
131. Umehara H, et al. Comprehensive diagnostic criteria for IgG4-related disease (IgG4-RD), 2011. Mod Rheumatol. 2012;22(1):21–30.

132. Hamano H, et al. IgG4-related disease – a systemic disease that deserves attension regardess of one's subspecialty. Intern Med. 2018;57(9):1201–7.
133. Ozaki Y, et al. Differentiation of autoimmune pancreatitis from suspected pancreatic cancer by floutrine-18 fluorodeoxylucose positron emission tomography. J Gastroenterol. 2008;43(2):144–51.
134. Zhang J, et al. Characterizing IgG4-related disease with ^{18}F-FDG PET/CT: a prospective cohort study. Eur J Nucl Med Mol Imaging. 2014;41(8):1624–34.
135. Tokue A, et al. Role of F-18 FDG PET/CT in assessing IgG4-related disease with inflammation of head and neck glands. Ann Nucl Med. 2015;29(6):499–505.
136. Krebs S, et al. IgG4-related kidney disease in a patient with history of breast cancer: findings on ^{18}F-FDG PET/CT. Clin Nucl Med. 2016;41(8):e388–9.
137. Nakatani K, et al. Utility of FDG PET/CT in IgG4-relayed systemic disease. Clin Radiol. 2012;67(4):297–305.
138. Kamisawa T, et al. IgG4-related disease. Lancet. 2015;385(9976):1460–71.
139. Nakajo M, et al. The efficacy of whole-body FDG PET or PET/CT for autoimmune pancreatitis and associated extrapancreatic autoimmune lesions. Eur J Nucl Med Mol Imaging. 2007;34(12):2088–95.
140. Oyama-Manabe N, et al. IgG4-related cardiovascular disease from the aorta to coronary artery: utility of multidetector CT and PET/CT in diagnosis and follow-up. Radiographics. 2018; https://doi.org/10.1148/rg.2018180049. 180049. [Epub ahead of print]
141. Yabusaki S, et al. Characteristics of immunoglobulin G4-related aortitis/periaortitis and periarteritis on flu orodeoxyglucose positron emission tomography/computed tomography co-registered with contrast-enhanced computed tomography. EJNMMI Res. 2017;7(1):20.